LBL-32846
UC-414

Lawrence Berkeley Laboratory
UNIVERSITY OF CALIFORNIA

Physics Division

To be published as a chapter in *Perspective on Higgs Physics*,
G. Kane, Ed., World Scientific, Singapore, 1992

Strong *WW* Scattering at the SSC and LHC

M.S. Chanowitz

July 1992

Prepared for the U.S. Department of Energy under Contract Number DE-AC03-76SF00098

DISCLAIMER

July 1992 LBL-32846

Strong WW Scattering at the SSC and LHC*

Michael S. Chanowitz

Theoretical Physics Group
Physics Division
Lawrence Berkeley Laboratory
1 Cyclotron Road
Berkeley, California 94720

To be published in *Perspective on Higgs Physics*, ed. G. Kane (World Scientific, Singapore).

*This work was supported by the Director, Office of Energy Research, Office of High Energy and Nuclear Physics, Division of High Energy Physics of the U.S. Department of Energy under Contract DE-AC03-76SF00098.

STRONG WW SCATTERING AT THE SSC AND LHC

MICHAEL S. CHANOWITZ
THEORETICAL PHYSICS GROUP, LAWRENCE BERKELEY LABORATORY
BERKELEY, CALIFORNIA 94720

Abstract

Signals and backgrounds for strong WW scattering at the SSC and LHC are considered. The Higgs mechanism without Higgs bosons is reviewed from the perspective of what it implies about the possibility of strong WW scattering. Complementarity of resonant signals in the $I = 1$ WZ channel and nonresonant signals in the $I = 2$ W^+W^+ channel is illustrated using a chiral lagrangian with a $J = 1$ WW "ρ" resonance. Results are presented for purely leptonic final states in the WZ, W^+W^+ , and ZZ channels. With a few exceptions, the signals are cleanly observable at the SSC with 10 fb^{-1} , and each model provides an observable signal in at least one gauge boson pair channel. Luminosity requirements are given for the LHC signals to meet the minimum significance criterion.

1. Introduction

This is an extraordinary moment for high energy physics. The successes of the previous decades have enabled us to construct a precise formulation of a fundamental problem — the origin of the weak gauge boson masses — so that without knowing the answer we are able to see quite clearly the nature of the experimental program that will lead us to it. In particular we know that with the necessary experimental facilities we will be able to discover a fifth force of nature and an associated set of new quanta that generate the W and Z boson masses. While we know neither the strength of the new force nor the mass of the associated quanta we do know the relationship between them and the energy domain within which their effects must become visible. This information is sufficient to guide the search.

The strategy of the search is based on the fact that the longitudinal polarization modes of the weak gauge bosons W and Z should really be counted among the new quanta associated with the fifth, electroweak symmetry breaking force. The Higgs

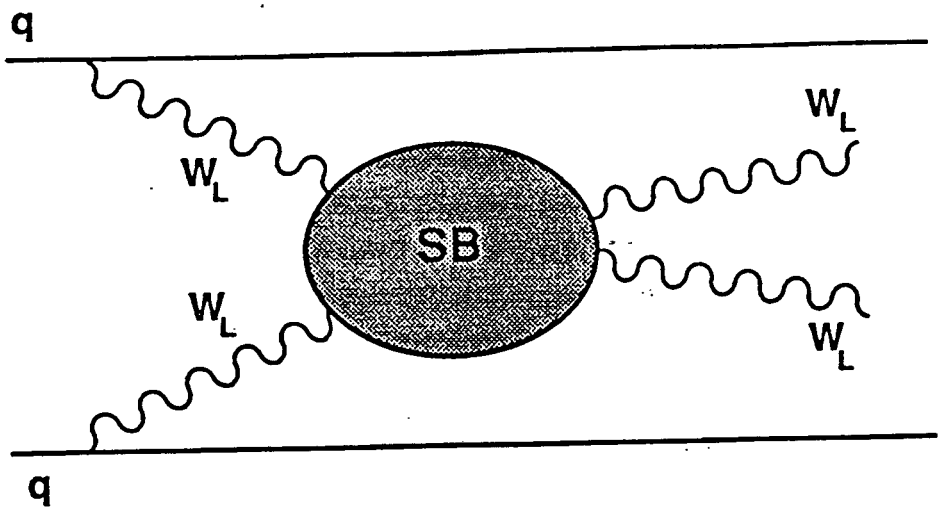

Figure 1.1 WW fusion via the interactions of the symmetry breaking sector.

mechanism implies that the longitudinal modes interact by means of the fifth force. If the fifth force is strong the contribution of the longitudinal modes causes WW scattering to become strong at energies above a TeV. It can then be studied at hadron or electron colliders with sufficient energy and luminosity, by means of the WW fusion process, figure 1.1. The ability to observe strong WW scattering is an essential component of a comprehensive search for the symmetry breaking mechanism, and it places the greatest demands on the collider energy and luminosity. The ability to observe strong WW scattering is essential to a "no-lose" search strategy, since other possible manifestations of the fifth force would appear at lower energy scales and be more readily observable.[1]. The absence of strong WW scattering above a TeV would unambiguously signal some form of new physics below a TeV.

The successes of the Standard Model are the basis for this extraordinary situation. The Standard Model is extremely reliable but is at the same time incomplete. It *predicts* the existence of the electroweak symmetry breaking (fifth) force for its consistent completion and implies the general framework that will guide the search. Like any prediction, this one may prove to be incorrect, though today it seems an unlikely possibility. However, its failure would constitute an arguably greater discovery than the discovery of the fifth force, since it would signify the failure of the Standard Model and would imply a deeper theory hidden until now behind the Standard Model, which would then require reinterpretation as an effective theory. This in effect generalizes the "no-lose" strategy, since any such breakdown of the standard model would become visible within the same energy region and by means of the same experimental

program that will lead us to the fifth force if the Standard Model is correct. I will focus here not on this possibility but on the more clearly defined scenario that follows if the Standard Model remains valid into the TeV domain.

In particular, I assume in this paper that the fifth force is strong *and* that it has no associated quanta below the TeV scale.* The guiding principle is the Higgs *mechanism* in its most general formulation, which does not require the existence of Higgs bosons. Section 2 is a review of the general features of the Higgs mechanism and especially the features that guide the search for a strong fifth force.

Assuming the fifth force is strong and has no associated light quanta, the most dramatic consequence would be WW resonance formation in the attractive channels at energies where the interaction is strong, probably between 1 and 3 TeV. The archetypical example is the techni-rho, ρ_{TC} , of technicolor models. The ρ_{TC} signals are estimated with a chiral lagrangian that incorporates the "ρ" in a chiral invariant manner,[25,26] consistent with the general symmetry properties required by the Higgs mechanism. The ρ_{TC} can be observed in the WZ channel in leptonic final states at the SSC with $E = 40$ TeV for 10 fb^{-1} integrated luminosity, corresponding to one experimental year at the design luminosity $\mathcal{L} = 10^{33}$ cm^{-2} sec^{-1}. For the LHC with 16 TeV the most difficult case ($N_{TC} = 2$) requires about 160 fb^{-1} to obtain a minimally significant signal. As an example of a vector meson resonance outside the technicolor framework (or if the large N_{TC} estimates fail) I also consider a 4 TeV "ρ" meson with width scaled from that of $\rho(770)$, that could not be detected at the SSC with 10 fb^{-1} but could be with 17 fb^{-1} and would require 570 fb^{-1} for observation at the LHC. These signals are presented in Section 4.

Though it seems unlikely, the lightest strong WW resonances could be much heavier than the 1 to 3 TeV that we naively expect, as in the example of the 4TeV "ρ" . In that case the best window on the fifth force is structureless strong WW scattering.[1] The most favorable channel is then likely to be like-charge WW pairs, W^+W^+ and W^-W^- , since they do not suffer from the $\bar{q}q$ annihilation background that dominates the other WW channels. The net branching ratio to like-charge electrons and/or muons is relatively large for a leptonic final state, about 5%, and the signature is striking — two isolated, like-sign, high p_T leptons in an otherwise "quiet" event.

There is a complementary relationship between the resonant and nonresonant

*If the fifth force is strong and does have associated quanta below 1 TeV, e.g., pseudo Goldstone bosons, the discussion of strong scattering given here may or may not be modified depending on the nature of the light quanta. See reference 2 for studies of this possibility.

signals in models with a two-body isovector "ρ" resonance resembling the ρ meson of QCD. For W_LW_L scattering in the $I = 0$ and $I = 2$ channels the t- and u-channel "ρ" exchanges interfere destructively with the low energy amplitudes predicted by low energy theorems[1,3] (which are a general consequence of the Higgs mechanism). Therefore W^+W^+ scattering (and $I = 0$ scattering also) is biggest precisely when the "ρ" production signal is smallest (because it is heavy and/or less strongly coupled). Models with big signals for W^+W^+ scattering are then most relevant when the "ρ" signal is most difficult to observe. Conversely, when t- and u-channel "ρ" exchange strongly suppresses the W^+W^+ signal, it is itself most easily observed directly in the $I = 1$ channel. This complementarity of the $I = 1$ and $I = 0,2$ channels is demonstrated in Section 3.2 in the chiral lagrangian framework.

Signals for strong W^+W^+ scattering are reviewed in Section 5. A powerful set of cuts[4,5,6] is used that are very effective in separating the signal from the backgrounds. The cuts favor the longitudinal polarization of the signal over the transverse polarization of the background, even though the W boson polarizations are not directly measurable in the relevant decay channel with two neutrinos, $W^+W^+ \to l^+\nu l^+\nu$. With one exception each model provides a very clear at the SSC with 10 fb^{-1} . The exception is the chiral lagrangian model for the $SU(4)_{TC}$ ρ_{TC} , which may or may not be observable (depending on the effect of higher order corrections on the signal efficiency for the "central jet veto") but is readily observable in the direct WZ resonance channel — illustrating the complementarity of the W^+W^+ and WZ channels. At the LHC about 100 fb^{-1} would be required to be assured of an observable signal for each model in at least one of the two channels.

Strong scattering in the ZZ channel is more difficult to observe because of the larger backgrounds. The ZZ channel is of special interest because it receives contributions from both W^+W^- and gluon-gluon fusion.[7] WW fusion probes W boson mass generation while gg fusion via a virtual $\bar{t}t$ pair probes the scale of the condensate that generates the top quark mass. It is commonly assumed in dynamical models of electroweak symmetry breaking that a single condensate generates both W and t masses, but it is possible, as is familiar in Higgs boson models, that the condensate responsible for m_t makes only a small contribution to M_W. It would be possible to probe for multiple condensates at the SSC with enhanced luminosity, $\gtrsim 50$ fb^{-1}, but probably not at the LHC. The conventional strong scattering signal — assuming a single condensate for M_W and m_t — just meets the minimum significance criterion at the SSC with 10 fb^{-1} , while 350 fb^{-1} are required at the LHC. These results are reviewed in Section 6.

The paper is organized as follows: the general framework — the Higgs mechanism without Higgs bosons — is reviewed in Section 2. Section 3 discusses the complementarity of resonant and nonresonant strong scattering signals, presents some specific models, and defines criteria for a minimally significant signal. Sections 4 - 6 review signals and backgrounds for the SSC and LHC: rho meson-like resonances in the WZ channel in Section 4 and nonresonant signals for W^+W^+ in Section 5 and ZZ in Section 6. Section 7 concludes with a brief overview of the the signals discussed in the previous Sections.

2. The Higgs Mechanism and its Implications

The Higgs mechanism does not require the existence of Higgs bosons. If the fifth force is strong we do not expect Higgs bosons to exist but do expect strong WW scattering to occur. Since it is the basis of our insight into strong WW scattering, I will sketch a general description of the Higgs mechanism in Section 2.1 that applies whether Higgs bosons exist or not. The implications for strong WW scattering are reviewed in the subsequent subsections: the Equivalence Theorem in 2.2, the WW low energy theorems in 2.3, and unitarity and the energy scale of strong WW scattering in 2.4.

2.1 The Generic Higgs Mechanism[8-10]

The basic ingredients of the Higgs mechanism are a gauge sector and a symmetry breaking sector,

$$\mathcal{L} = \mathcal{L}_{\text{gauge}} + \mathcal{L}_5 \ . \tag{2.1}$$

$\mathcal{L}_{\text{gauge}}$ is an unbroken *locally symmetric = gauge invariant* theory, describing massless gauge bosons that are transversely polarized, just like the photon. For instance, for $SU(2)_L \times U(1)_Y$ gauge symmetry the gauge bosons are a triplet $\vec{W} = W_1, W_2, W_3$ corresponding to the generators $\vec{T}_L$ and a singlet gauge boson X corresponding to the hypercharge generator Y. $\mathcal{L}_5$ is the symmetry breaking Lagrangian that describes the dynamics of the fifth force and the associated quanta. If $\mathcal{L}_5$ did not exist, the unbroken $SU(2)_L$ nonabelian symmetry would give rise to a force that would confine quanta of nonvanishing $\vec{T}_L$ charge, such as left-handed electrons and neutrinos.

In the generic Higgs mechanism $\mathcal{L}_5$ breaks the *local* (or *gauge*) symmetry of $\mathcal{L}_{\text{gauge}}$. To do so $\mathcal{L}_5$ must possess a *global* symmetry G that breaks spontaneously to a subgroup H,

$$G \to H. \tag{2.2}$$

In the electroweak theory we do not yet know either of the groups G or H,

$$G = ? \tag{2.3a}$$

$$H = ? \tag{2.3b}$$

We want to discover what they are and beyond that we want to discover the symmetry breaking sector

$$\mathcal{L}_5 = ? \tag{2.4}$$

including the mass scale of its spectrum

$$M_5 = ? \tag{2.5}$$

and the interaction strength

$$\lambda_5 = ? \tag{2.6}$$

We do already know one fact about G and H: G must be at least as big as $SU(2)_L \times U(1)_Y$ or $\mathcal{L}_5$ would *explicitly* (as opposed to *spontaneously*) break the $SU(2)_L \times U(1)_Y$ gauge symmetry. Similarly H must be at least as big as $U(1)_{EM}$ or the theory after spontaneous breakdown will not accommodate the unbroken gauge symmetry of QED. That is, in order to be consistent with the desired pattern of breaking for the *local* symmetry

$$SU(2)_L \times U(1)_Y \rightarrow U(1)_{EM} \tag{2.7}$$

the spontaneous breaking of the *global* symmetry of $\mathcal{L}_5$

$$G \rightarrow H \tag{2.8}$$

is constrained by

$$G \supset SU(2)_L \times U(1)_Y \tag{2.9}$$

$$H \supset U(1)_{EM} \tag{2.10}$$

There are two steps in the Higgs mechanism. The first has nothing to do with gauge symmetry—it is just the spontaneous breaking of a global symmetry as explained by the Goldstone theorem. By *spontaneous* symmetry breaking $G \rightarrow H$ we mean that

$$G = \text{ global symmetry of } \textit{interactions} \text{ of } \mathcal{L}_5 \tag{2.11a}$$

while

$$H = \text{ global symmetry of the } \textit{ground-state} \text{ of } \mathcal{L}_5 \ . \tag{2.11b}$$

That is, the dynamics of $\mathcal{L}_5$ are such that the state of lowest energy (the *vacuum* in quantum field theory) has a smaller symmetry group than the symmetry of the force laws of the lagrangian. Goldstone's theorem tells us that for each broken generator of G the spectrum of $\mathcal{L}_5$ contains a massless spin zero particle or Goldstone boson,

$$\begin{aligned} &\#\text{ of massless scalars} \\ &\quad = \#\text{ of broken symmetry axes} \\ &\quad = \text{dimension } G - \text{dimension H} \\ &\quad = \#\text{ of energetically flat directions in field space.} \end{aligned} \tag{2.12}$$

The last line is the clue to the proof of the theorem: masses arise from terms that are quadratic in the fields,

$$\mathcal{L}_{\text{mass}} = -\frac{1}{2}m^2\phi^2, \tag{2.13}$$

so a field direction that is locally flat in energy (i.e., goes like ϕ^n with $n \geq 3$) corresponds to a massless mode.

The essential features are the symmetries of the lagrangian (G) and the ground state (H). Elementary scalars are *not* essential: if necessary Nature will make composite massless scalars. She has (almost) already done so on at least one occasion: we believe on the basis of strong theoretical and experimental evidence that QCD with two (almost) massless quarks is an example, with the pion isotriplet the (almost) Goldstone bosons. The initial global (flavor) symmetry of two flavor QCD in the $m_u = m_d = 0$ limit is

$$G = SU(2)_L \times SU(2)_R \tag{2.14}$$

since we could perform separate isospin rotations on the right and left chirality u and d quarks. The ground state has a nonvanishing expectation value for the bilinear operator

$$\langle \bar{u}_L u_R + \bar{d}_L d_R + h.c. \rangle_0 \neq 0 \tag{2.15}$$

where $h.c.$ = hermitian conjugate. The condensate (2.15) breaks the global symmetry spontaneously, $G \to H$, where

$$H = SU(2)_{L+R} \tag{2.16}$$

is the ordinary isospin group of nuclear and hadron physics. That is, (2.15) is not invariant under independent rotations of left and right helicity quarks but only under rotations that act equally on left and right helicities. In this example dim $G = 6$ and dim $H = 3$ so we expect $6 - 3 = 3$ Goldstone bosons. In nature we believe they are the pion triplet, π^+, π^-, π^0, which are much lighter than typical hadrons because the

u and d quark masses are very small, of order 10 MeV. (I refer to the "current" quark masses, the parameters that appear in the QCD Lagrangian.)

In the first step we considered only the global symmetry breakdown induced by $\mathcal{L}_5$ — Goldstone's theorem. Now we come to the second step, which involves the interplay of $\mathcal{L}_5$ with $\mathcal{L}_{\text{gauge}}$. The essential point of the Higgs mechanism is that when a spontaneously broken generator of $\mathcal{L}_5$ coincides with a generator of a gauge invariance of $\mathcal{L}_{\text{gauge}}$, the associate Goldstone boson w and massless gauge boson W mix to form a massive gauge boson. The number of degrees of freedom are preserved, since the Goldstone boson disappears from the physical spectrum while the gauge boson acquires a third (longitudinal) polarization state. Like the first step this is a general phenomenon that depends only on the nature of the global and local symmetries, regardless of whether there are elementary scalar particles in the theory.

Suppose the Goldstone boson w couples to one of the gauge currents, with a coupling strength f with the dimension of a mass,

$$\langle 0|J^{\mu}_{\text{gauge}}|w(p)\rangle = \frac{i}{2} f p^{\mu} \tag{2.17}$$

f is analogous to F_π, the pion decay constant, that specifies the coupling of the pion to the axial isospin current,

$$\langle 0|J^{\mu}_{5}|\pi(p)\rangle = iF_\pi p^{\mu} \tag{2.18}$$

Equation (2.17) means that the current contains a term linear in w,

$$J^{\mu}_{\text{gauge}}(x) = \frac{1}{2} f \partial^{\mu} w(x) + \cdots \tag{2.18}$$

In the lagrangian J^{μ}_{gauge} is by definition coupled to the gauge boson W^{μ},

$$\mathcal{L}_{\text{gauge}} = g W_{\mu} J^{\mu}_{\text{gauge}} + \cdots \tag{2.19}$$

where g is the dimensionless gauge coupling constant. Substituting Eq. (2.17) we find

$$\mathcal{L}_{\text{gauge}} = \frac{1}{2} g f W_{\mu} (\partial^{\mu} w) \ldots \tag{2.20}$$

which shows that W_μ mixes in the longitudinal (parallel to $\vec{p}$) direction with the would–be Goldstone boson w.

We can use (2.20) to compute the W mass.[8–10] In the absence of symmetry breaking the W is massless and transversely polarized. Therefore as in QED we can write its propagator in Landau gauge,

$$D_0^{\mu\nu} = \frac{-i}{k^2}(g^{\mu\nu} - \frac{k^{\mu}k^{\nu}}{k^2}) \tag{2.21}$$

In higher orders the propagator is the sum of the geometric series due to "vacuum polarization", i.e., all states that mix with the gauge current. The vacuum polarization tensor is defined as

$$\begin{aligned}\Pi^{\mu\nu}(k) &= -\int d^4k e^{-ik\cdot x}\langle TJ^\mu(x)J^\nu(0)\rangle_0 \\ &= i\frac{g^2f^2}{4}(g^{\mu\nu}-\frac{k^\mu k^\nu}{k^2})\frac{1}{k^2}+\cdots \end{aligned} \tag{2.22}$$

In Eq. (2.22) I have indicated explicitly the contribution from the Goldstone boson pole: the factor $1/k^2$ is just the massless propagator and the factor $(gf/2)^2$ can be recognized from Eq. (2.20). The $g^{\mu\nu}$ term is present since gauge invariance requires current conservation, $k_\mu\Pi^{\mu\nu}=0$. Since it is a constant term with no absorptive part, its presence does not change the spectrum of the theory. (In theories with elementary scalars it arises automatically from the "seagull" interaction given by the Feynman rules.)

Finally we compute the W propagator from the geometric series

$$\begin{aligned}D^{\mu\nu} &= (D_0 + D_0\Pi D_0 + \ldots)^{\mu\nu} \\ &= -\frac{i}{k^2}\left(g^{\mu\nu}-\frac{k^\mu k^\nu}{k^2}\right)\left(1+\frac{g^2f^2}{4k^2}+\cdots\right) \\ &= -i\left(g^{\mu\nu}-\frac{k^\mu k^\nu}{k^2}\right)\frac{1}{k^2}\frac{1}{1-\frac{g^2f^2}{4k^2}} \\ &= -i\frac{g^{\mu\nu}-\frac{k^\mu k^\nu}{k^2}}{k^2-\frac{g^2f^2}{4}}. \end{aligned} \tag{2.23}$$

The massless Goldstone boson pole then induces a pole in the gauge boson propagator(!),

$$M_W = \frac{1}{2}gf. \tag{2.24}$$

From the measured value of the Fermi constant,

$$G_F = \frac{g^2}{4\sqrt{2}M_W^2} = \frac{1}{\sqrt{2}f^2} \tag{2.25}$$

we learn that

$$f \simeq 250GeV. \tag{2.26}$$

Customarily instead of f we refer to $v \equiv f$, the so–called vacuum expectation value. This custom, which I will also follow (though in general it is not really correct)

derives from theories with elementary scalar fields where $v \equiv f$ is both the coupling strength of the Goldstone boson w to $J_{\rm gauge}$, as in (2.17), and is also the value of the Higgs boson field in the ground state (i.e., the Higgs boson vacuum condensate). However the derivation just reviewed shows that there is no need for a Higgs boson to exist. The condensate that breaks the symmetry may be that of a composite operator, e.g., Eq. (2.15), which in general has no simple relationship to the parameter $f \equiv v$ defined in (2.17). For instance, in QCD there is no trivial relationship between F_π and $\langle \bar{u}u + \bar{d}d \rangle_0$ (although there is a nontrivial relation involving also the quark and pion masses).

2.2 The Equivalence Theorem

The equivalence theorem is very useful for analyzing the implications of the Higgs mechanism for strong WW scattering. In the U (unitary) gauge the Goldstone boson fields $\vec{w}$ are absent from the Lagrangian. In R (renormalizable) gauges they do appear in $\mathcal{L}_5$ and in the Feynman rules, though gauge invariance ensures that are not in the physical spectrum. Since they engender the longitudinal gauge boson modes, W_L and Z_L, it is plausible that W_L and Z_L interactions reflect the dynamics of $\vec{w}$. The equivalence theorem is the precise statement of this proposition,

$$\mathcal{M}(W_L(p_1), W_L(P_2), \ldots) = \mathcal{M}(w(p_1), w(p_2), \ldots)_R + O\left(\frac{M_W}{E_i}\right). \tag{2.27}$$

As indicated the equality holds up to corrections of order M_W/E_i.

We will see that the equivalence theorem is useful in the derivation of the $W_L W_L$ low energy theorems and that it is also a useful source of intuition for the possible dynamics of strong WW scattering. In addition, it greatly simplifies perturbative computations. For instance, the evaluation of heavy Higgs boson production via WW fusion in unitary gauge requires evaluation of many diagrams with "bad" high energy behavior that cancel to give the final result. But to leading order in the strong coupling $\lambda = m_H^2/2v^2$ it suffices using the equivalence theorem to compute just a few simple diagrams. The result embodies the cancellations of many diagrams in unitary gauge and trivially has the correct high energy behavior. It is very accurate for energies above 1 TeV (of order 1 % or better).

A simple example may be instructive. Consider the decay of a heavy higgs boson to a pair of longitudinally polarized gauge bosons $W_L^+ W_L^-$. In unitary gauge the $HW_L^+W_L^-$ amplitude is

$$\mathcal{M}(H \to W_L^+ W_L^-) = g M_W \epsilon_L(p_1) \cdot \epsilon_L(p_2). \tag{2.28}$$

For $m_H \gg M_W$ we neglect terms of order M_W/m_H, so that $\epsilon_L^\mu(p_i) \cong p_i/M_W$ and similarly from $m_H^2 = (p_1 + p_2)^2 \cong 2p_1 \cdot p_2$ we find

$$\mathcal{M}(H \to W_L^+ W_L^-) = g\frac{m_H^2}{2M_W} + O\left(\frac{M_W}{m_H}\right). \tag{2.29}$$

In a renormalizable gauge the corresponding amplitude can be read off (taking care with factors of 2) from the Hww vertex in the Higgs potential, with the result

$$\mathcal{M}(H \to w^+ w^-) = 2\lambda v. \tag{2.30}$$

Using the relations $M_W = \frac{1}{2}gv$ and $\lambda = m_H^2/2v^2$ we see that Eqs. (2.29) and (2.30) are indeed equal up to $O(M_W/m_H)$ corrections.

The theorem was first proved in tree approximation[11] and used in a variety of calculations.[12–14] Reference 13 contains a proof to all orders which does not however apply to matrix elements with more than one external W_L. A proof to all orders in both $\mathcal{L}_5$ and $\mathcal{L}_{\text{gauge}}$ was given in reference 1 and alternative treatments of a portion of that proof have been given in references 15 - 17. The fact that the theorem holds to all orders in the strong interactions of $\mathcal{L}_5$ is crucial for its applicability to strong WW scattering. Bagger and Schmidt[17] have questioned whether the theorem holds to all orders in the electroweak gauge interactions. For an Abelian gauge theory Kilgore[18] has recently demonstrated a simple renormalization prescription that insures the validity of the theorem to all orders in both the gauge and symmetry breaking interactions. His treatment clarifies the gauge and renormalization-prescription dependence of the theorem. Similar conclusions have also been reached by He, Kuang, and Li[19] in the nonabelian case.

2.3 Low Energy Theorems

Using the equivalence theorem and the general properties of the Higgs mechanism described in Section 2.1 we can derive the low energy theorems for $W_L W_L$ scattering that in turn set the scale for the onset of strong WW scattering. The symmetry breaking pattern of $\mathcal{L}_5$, $G \to H$, implies low energy theorems for the Goldstone bosons, which imply $W_L W_L$ low energy theorems by means of the equivalence theorem. In general the low energy theorems are determined by the groups G and H and by two parameters, the vacuum expectation value v and the ρ parameter, $\rho = M_W^2/(M_Z^2 \cos^2\theta_W)$. Recall that we assume that there are no light quanta in $\mathcal{L}_5$ other than w and z. If there are other light quanta in $\mathcal{L}_5$ they may or may not modify the low energy theorems.[3]

Low energy theorems for the $2 \to 2$ scattering of Goldstone bosons were first derived by Weinberg[20] for pion-pion scattering. Identifying the pion isotriplet with the almost-Goldstone bosons of spontaneous flavor symmetry breaking $SU(2)_L \times SU(2)_R \to SU(2)_{L+R}$ in hadron physics, Weinberg showed for example that

$$\mathcal{M}(\pi^+\pi^- \to \pi^0\pi^0) = \frac{s}{F_\pi^2} \tag{2.31}$$

where $F_\pi = 93$ MeV is the pion decay constant defined in Eq. (2.18). Equation (2.31) neglects $O(m_\pi^2)$ corrections (which are in fact calculable to leading order and were computed by Weinberg) and is valid at low energy, defined as

$$s \ll \text{minimum}\{m_\rho^2, (4\pi F_\pi)^2\}. \tag{2.32}$$

The low energy theorems can be derived by current algebra or effective lagrangian methods. The proof has two important features:

- it is valid to all orders in the Goldstone boson self–interactions. This is crucial since those interactions may be strong (as they are for the pion example) so that perturbation theory is a non-starter,
- we needn't be able to solve the dynamics or even to know the lagrangian of the theory. In fact the $\pi\pi$ low energy theorems were derived in 1966 before QCD was discovered. (And we still don't know today how to compute $\pi\pi$ scattering directly in QCD.)

The current algebra/symmetry method was important in the path followed in the 1960's that led in the early 1970's to the discovery that $\mathcal{L}_{HADRON} = \mathcal{L}_{QCD}$. It is similarly useful today in our search for $\mathcal{L}_5$.

If $G = SU(2)_L \times SU(2)_R$ and $H = SU(2)_{L+R}$ as in QCD, then we can immediately conclude, just as in Eq. (2.31) that[1]

$$\mathcal{M}(w^+w^- \to zz) = \frac{s}{v^2} \tag{2.33}$$

at low energy,

$$s \ll \text{minimum}\{M_5^2, (4\pi v)^2\}, \tag{2.34}$$

as in eq. (2.32). Here M_5 is the typical mass scale of $\mathcal{L}_5$ and $v \simeq \frac{1}{4}$ TeV. More generally, electroweak gauge invariance requires Eqs. (2.9) and (2.10) from which we can deduce the more general result[3]

$$\mathcal{M}(w^+w^- \to zz) = \frac{1}{\rho}\frac{s}{v^2}. \tag{2.35}$$

Equation (2.35) is arguably more soundly based than (2.31) was in 1966, since (2.35) is a general consequence of gauge invariance and the Higgs mechanism while (2.31) was based on inspired guesswork as to the symmetries underlying hadron physics. The low energy theorems are proved by three different methods[3]: perturbatively, by a current algebra derivation similar to Weinberg's, and by the chiral lagrangian method.

We can next use the equivalence theorem, Eq. (2.27), to turn Eq. (2.35) into a physical statement about longitudinal gauge boson scattering. In particular we have

$$\mathcal{M}(W_L^+W_L^- \to Z_LZ_L) = \frac{1}{\rho}\frac{s}{v^2} \tag{2.36}$$

for an energy domain circumscribed by Eqs. (2.34) and (2.27) as

$$M_W^2 \ll s \ll \text{minimum}\{M_5^2, (4\pi v)^2\}. \tag{2.37}$$

The window (2.37) may or may not exist in nature, depending on whether $M_5 \gg M_W$.

In addition to Eq. (2.36) there are two other independent amplitudes which may be chosen to be W^+W^- and ZZ elastic scattering. Their low energy theorems are:

$$\mathcal{M}(W_L^+W_L^- \to W_L^+W_L^-) = -\left(4 - \frac{3}{\rho}\right)\frac{u}{v^2}, \tag{2.38}$$

$$\mathcal{M}(Z_LZ_L \to Z_LZ_L) = 0. \tag{2.39}$$

There are in addition four others that follow by crossing symmetry:

$$\mathcal{M}(W_L^\pm Z_L \to W_L^\pm Z_L) = \frac{1}{\rho}\frac{t}{v^2}, \tag{2.40}$$

$$\begin{aligned}\mathcal{M}(W_L^+W_L^+ &\to W_L^+W_L^+) \\ &= \mathcal{M}(W_L^-W_L^- \to W_L^-W_L^-) = -(4 - \frac{3}{\rho})\frac{s}{v^2}.\end{aligned} \tag{2.41}$$

2.4 Unitarity and the Scale of Strong WW Scattering

The threshold energy dependence predicted by the low energy theorems would eventually violate unitarity unless damped. In fact, the low energy theorems are identical with the famous "bad" high energy behavior that the Higgs mechanism was invented to cure — this emerges most clearly in the perturbative derivation.[3] Within the Higgs mechanism it is the task of $\mathcal{L}_5$ to cut off the growing amplitudes Eqs. (2.36-2.41). Unitarity implies a rigorous upper bound on the energy at which this must

occur. The use of unitarity here is identical to that of Lee and Yang[21] and of Ioffe, Okun, and Rudik[22] who used the growing behavior of fermion-fermion scattering in Fermi's four-fermion weak interaction lagrangian (also proportional to $G_F s \propto s/v^2$!) to bound the scale at which Fermi's theory must break down — essentially a bound on the mass of the W boson. In fact that bound is precisely half the value of the bound given below for the scale of the symmetry breaking physics.

In particular we use partial wave unitarity. The partial wave amplitudes for the Goldstone scalars (or for the zero helicity, longitudinal gauge bosons) are

$$a_J(s) = \frac{1}{32\pi} \int d(\cos\theta) P_J(\cos\theta) \mathcal{M}(s,\theta) \tag{2.42}$$

where θ is the center of mass scattering angle. Partial wave unitarity then requires

$$|a_J(s)| \leq 1. \tag{2.43}$$

Putting $\rho = 1$ we then find

$$a_0(W_L^+ W_L^- \to Z_L Z_L) = \frac{s}{16\pi v^2} \leq 1 \tag{2.44}$$

so that the interactions of $\mathcal{L}_5$ must intervene to damp the absolute value of the amplitude at a scale Λ_5 bounded by

$$\Lambda_5 \leq 4\sqrt{\pi} v \simeq 1.75\ TeV. \tag{2.45}$$

At the cutoff, $s \cong O(\Lambda_5)$, the $J = 0$ wave is

$$a_0(\Lambda_5) \cong \frac{\Lambda_5^2}{16\pi v^2} \tag{2.46}$$

which relates the strength of the interaction and the energy scale of the new physics. If $\Lambda_5 \lesssim \frac{1}{2}$ TeV then $a_0(\Lambda_5) \lesssim 1/4\pi$, well below the unitarity limit. Then $\mathcal{L}_5$ has a weak coupling and can be analyzed perturbatively. For $\Lambda_5 \gtrsim 1$ TeV, we have $a_0(\Lambda_5) \gtrsim 1/3$, which is close to saturation. Then $\mathcal{L}_5$ is a strong interaction theory requiring nonperturbative methods of analysis.

Though not rigorously demonstrable, the most likely possibility is that Λ_5 is of the order of the typical mass scale M_5 of the quanta of $\mathcal{L}_5$,

$$\Lambda_5 \cong M_5. \tag{2.47}$$

We can illustrate this with two significant examples. The first is the Weinberg–Salam model, in which s–channel Higgs exchange provides the cutoff. Assume that $m_H \gg M_W$ but that m_H is small enough that perturbation theory is not too bad —

say $m_H \simeq 700$ GeV so that $\lambda/4\pi^2 = m_H^2/8\pi v^2 \simeq 1/10$. To leading order the $J = 0$ partial wave is

$$a_0(s) = \frac{s}{16\pi v^2} - \frac{s}{16\pi v^2}\,\frac{s}{s - m_H^2} \tag{2.48}$$

where the first term arises from $\mathcal{L}_{\text{gauge}}$ and the second from the s-channel Higgs boson exchange due to $\mathcal{L}_5$ now assumed to be the Weinberg-Salam Higgs sector. For $s \ll m_H^2$ the first term dominates, giving the low energy theorem, Eq. (2.44), as it must. But for $s \gg m_H^2$ the two terms combine to give

$$a_0\Big|_{s \gg m_H^2} = \frac{m_H^2}{16\pi v^2}. \tag{2.49}$$

Comparing Eq. (2.49) with (2.46) we see that (2.47) is indeed verified, i.e., $\Lambda_5 \cong m_H$.

Consider next a strongly-coupled example. In this case we expect to approximately saturate the unitarity bound,

$$\Lambda_5 \cong 4\sqrt{\pi}v \cong O(2)TeV. \tag{2.50}$$

We cannot actually compute M_5 in this case but we can relate the problem to one that has been studied experimentally. In hadron physics the analogous saturation scale from the $\pi\pi$ low energy theorems is

$$\Lambda_{\text{Hadron}} \cong 4\sqrt{\pi}f_\pi \cong 650MeV \tag{2.51}$$

which indeed coincides with the mass scale of the lightest (non-Goldstone boson) hadrons, e.g., $m_\rho = 770$ MeV. The coincidence is not surprising: we expect resonances to form when scattering amplitudes become strong, as they do at the energy scale of the unitarity bound.

The general lesson can be extracted from the Higgs boson example: the cutoff occurs at a scale $s \simeq M_5^2$ characteristic of $\mathcal{L}_5$, and at energies $\sqrt{s} \geq M_5$ the magnitude of the amplitude is of order

$$|a_0(s)| \cong O\left(\frac{M_5^2}{(1.8\text{TeV})^2}\right). \tag{2.52}$$

More precisely, M_5 is *the mass scale of the quanta that make the condensate that generates M_W and M_Z.*

For $M_5 \ll 1.8$ TeV, the Lagrangian $\mathcal{L}_5$ is weak, WW scattering is never strong, and the amplitudes are cut off by the exchange of narrow $J = 0$ bosons, i.e., *Higgs* bosons. In that case M_5 is an appropriately weighted (by vev) average of the Higgs boson masses,

$$M_5 = \sqrt{\langle m_H^2 \rangle}. \tag{2.53}$$

If $M_5 \geq 1$ TeV then $\mathcal{L}_5$ is strong and Eq. (2.52) shows that there will be strong WW scattering above 1 TeV. We do not then necessarily expect a Higgs boson but do expect a complex strongly interacting spectrum. We expect resonances to appear at the mass scale M_5 at which the partial wave amplitudes become strong, $|a_J(M_5^2)| \sim O(1)$, which implies $M_5 \sim 1 - 3$ TeV. As discussed in Section 4 strong two body resonances in that mass region would be observable with 10 fb^{-1} at the SSC, and signals meeting minium significance criteria could be obtained at the LHC with an order of magnitude greater luminosity. If the resonances are unexpectedly heavier we can still probe $\mathcal{L}_5$ by means of nonresonant strong WW scattering at $\sqrt{s} \geq 1$ TeV, the subject of Sections 5 and 6.

3. Strong WW Scattering Models and Complementarity

The ET-EWA approximation[1] is the basis of most studies of strong WW scattering in pp colliders. "ET-EWA" refers to the combined use of the Equivalence Theorem and the effective W approximation. As discussed in Section 2.2, the equivalence theorem allows us to model the basic W_LW_L subprocess by models of ww Goldstone boson scattering, provided we are not too close to the WW threshold where $O(M_W/E)$ corrections are large. To obtain predictions for WW scattering in pp or e^+e^- collisions the models for W_LW_L scattering are then convoluted with the W_LW_L effective luminosity as given by the effective W approximation. This introduces two additional sources of $O(M_W/E)$ corrections: first, the EWA intrinsically neglects $O(M_W/E)$ corrections and second, the "initial state" W_LW_L pair is off mass shell of order $O(M_W/E)$.

3.1 Effective W Approximation

The effective W approximation is analogous to the effective photon approximation of Weiszacker and Williams. It provides an effective luminosity distribution for the probability to find colliding "beams" of longitudinally polarized gauge bosons within the colliding quark "beams" produced at a pp collider or within the e^+e^- beams at an e^+e^- collider. For incident fermions f_1 and f_2 the effective luminosity for longitudinally polarized gauge bosons V_1 and V_2 is

$$\left.\frac{\partial \mathcal{L}}{\partial z}\right|_{V_1V_2/f_1f_2} = \frac{\alpha^2\chi_1\chi_2}{\pi^2 \sin^4\theta_W}\frac{1}{z}\left[(1+z)\ln\left(\frac{1}{z}\right) - 2 + 2z\right] \tag{3.1}$$

where $z \equiv s_{VV}/s_{ff}$ and the χ_i are the f_i - V_i couplings, e.g., $\chi_W = 1/4$ for all fermions, $\chi_{Zu\bar{u}} = (1 + (1 - \frac{8}{3}\sin^2\theta_W)^2)/16\cos^2\theta_W$, etc .... Equation (3.1) must be convoluted

with the desired V_1V_2 subprocess cross section and also with the quark distribution functions in the case of pp collisions,

$$\sigma(pp \to \cdots) = \int_\tau \left.\frac{\partial \mathcal{L}}{\partial \tau}\right|_{qq/pp} \cdot \int_x \sum_{V_L} \left.\frac{\partial \mathcal{L}}{\partial x}\right|_{V_LV_L/qq} \cdot \sigma(V_LV_L \to \cdots) \tag{3.2}$$

The effective W approximation has been compared with analytical and numerical evaluations of Higgs boson production. The analytical calculations[24] show good agreement for $WW \to H$ for $m_H \geq 500$ GeV, with errors $\lesssim O(10\%)$ and decreasing with m_H and $\sqrt{s}$, while for the relatively less important process $ZZ \to H$ the errors are roughly twice as large. Above 1 TeV the errors are very small.

3.2 Strong Scattering Models, $\pi\pi$ Scattering Data and Complementarity

The possibility that strong WW resonances may be heavier than the expected 1-3 TeV domain motivates a class of models in which the threshold amplitudes are unitarized in a gradual, gentle fashion. The most naive example is the linear model,[1] that takes the threshold amplitudes, Eqs. (2.36 - 2.41), which are purely real, as a model of the absolute value of the partial wave amplitudes below the unitarity limit and sets the absolute value of the partial wave amplitudes equal to one at higher energies. For instance, for the $I, J = 0, 0$ partial wave the model is

$$|a_{00}| = \frac{s}{16\pi v^2}\theta(16\pi v^2 - s) + \theta(s - 16\pi v^2). \tag{3.3}$$

The discontinuity in the derivative is unphysical but the model is nonetheless a potentially useful guide to the *magnitude* of certain partial waves. It gives a surprisingly good description of the pion scattering data in the $I = J = 0$ channel, as shown below.

The standard K-matrix unitarization is another smooth extrapolation of the low energy theorems.† In the K-matrix method a partial wave amplitude is specified in terms of its reciprocal, $1/a_J$. Partial wave unitarity is equivalent to the statement that

$$Im(a_J^{-1}) = -1 \tag{3.4}$$

so that a unitary a_J can be completely specified by specifying the real part of a_J^{-1}. For instance, for the isoscalar channel we choose

$$Re(a_{00}^{-1}) = \frac{16\pi v^2}{s}, \tag{3.5}$$

†K-matrix models of W_LW_L scattering were first considered in reference 4.

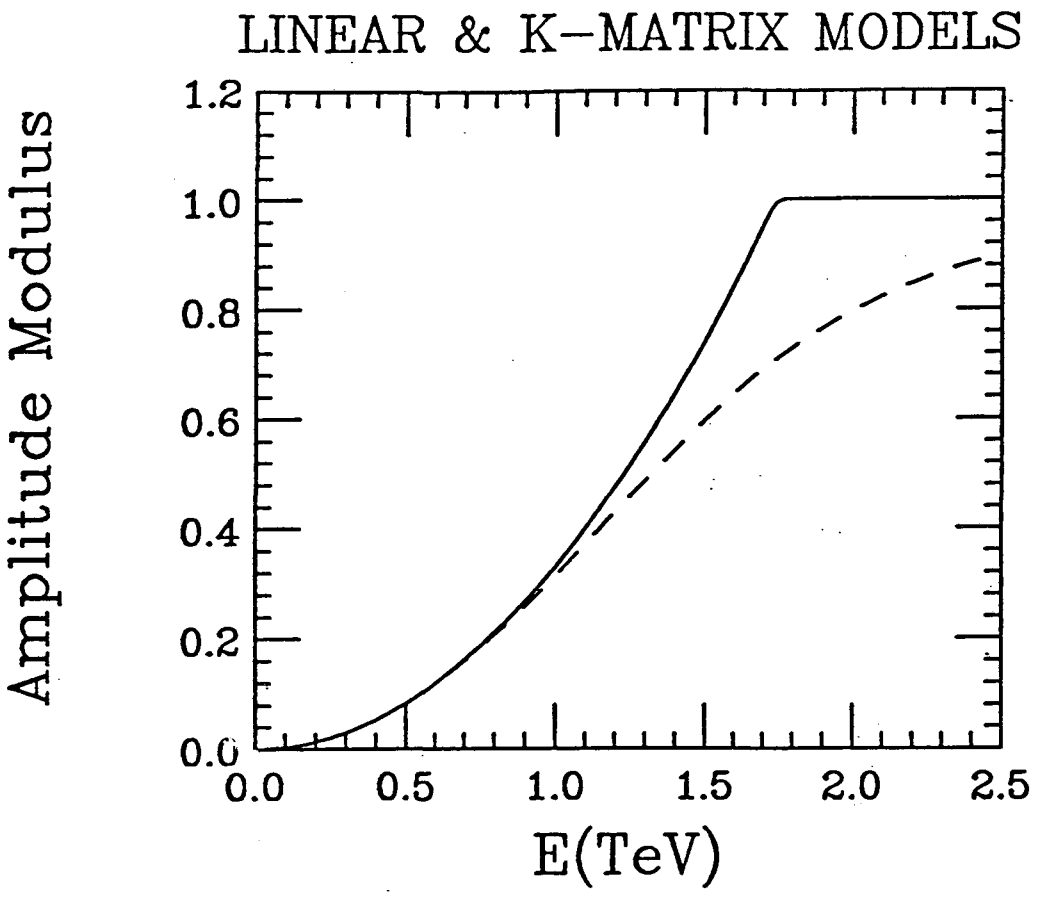

Figure 3.1 Modulus of the $IJ = 00$ partial wave, $|a_{00}|$, in the linear and K-matrix models.

which is the inverse of the threshold amplitude given by the low energy theorem (for $\rho = 1$). The K-matrix amplitude is then

$$a_{00} = \frac{s}{16\pi v^2}\left(1 + i\frac{s}{16\pi v^2}\right)^{-1}. \tag{3.6}$$

The linear and K-matrix models for the 00 channel of $W_L W_L$ scattering are shown in figure 3.1.

For the like-charge $I, J = 2, 0$ channel the analogous model amplitudes are

$$|a_{20}| = \frac{s}{32\pi v^2}\theta(32\pi v^2 - s) + \theta(s - 32\pi v^2) \tag{3.7}$$

and

$$a_{20} = -\frac{s}{32\pi v^2}\left(1 + i\frac{s}{32\pi v^2}\right)^{-1}. \tag{3.8}$$

A variety of other strong scattering models have also been considered. The N/D method has been applied to interpret the theory of the ultraheavy Higgs boson.[30]

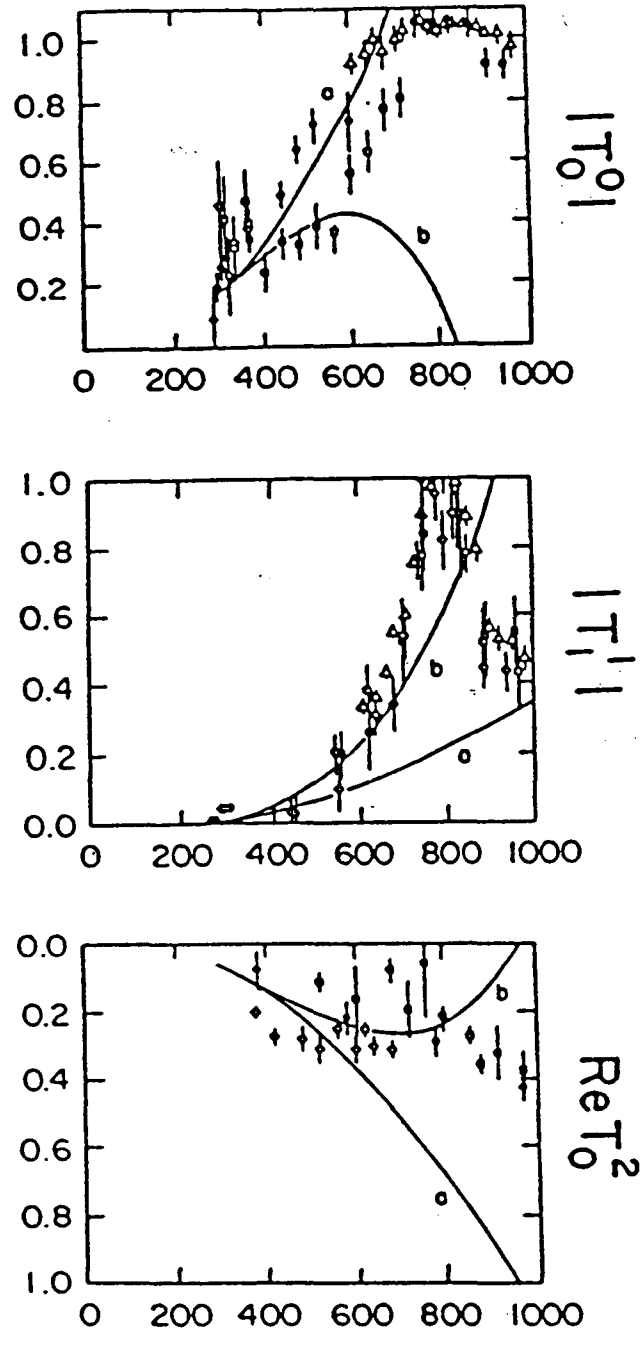

Figure 3.2 Compilation of $\pi\pi$ scattering data from reference 28.

The resulting isoscalar partial wave amplitude resembles but is considerably larger than that of the linear model. Chiral lagrangians[31–33] including higher dimension operators and loop contributions to maintain unitarity[‡] are an interesting way to

[‡]The latter without the former were studied by Cheyette and Gaillard[31a] while the former without the latter were studied by Golden[31b].

parameterize the model amplitudes. However the significance of the $O(s^2)$ corrections is circumscribed by the fact that when they become very important they also become untrustworthy, since their importance signals the breakdown of the chiral expansion.

It is instructive to compare the linear model with pion scattering data in the three leading partial waves, $IJ = 00,\ 11,\ 20$. In Figure 3.2 from reference 28 the solid line labeled *a* represents the linear model (with leading pion mass corrections included). It is a surprisingly good fit to the 00 channel, including even the "discontinuity" in the slope at saturation and the continuing saturation at 1 for higher energy. The scale at which saturation occurs, $4\sqrt{\pi}F_\pi = 650$ MeV, is the analogue of the $4\sqrt{\pi}v = 1.75$ TeV scale identified with Λ_5 in Eq. (2.45).

The $\pi\pi$ scattering data for the $I = 1$ and $I = 2$ amplitudes illustrates the complementarity of the resonant and nonresonant channels. In the $I = 1$ channel the linear model drastically underestimates the magnitude of the amplitude because of the ρ resonance. In the $I = 2$ channel it tracks the data fairly well until about $\simeq 600$ MeV (analogous to $\simeq 1.6$ TeV in W_LW_L scattering) where it begins to overestimate the data for the magnitude of the amplitude. This is *also* a consequence of the ρ resonance, in this case the force due to the t- and u-channel ρ exchange, which interferes destructively with the threshold amplitude as discussed in Section 3.2. If $\rho(770)$ were heavier and/or less strongly coupled to $\pi\pi$, the linear model would be a better fit to the data in both the isovector and isotensor channels. The a_{11} amplitude would then be smaller while the a_{20} amplitude would be bigger!

The remarkable agreement of the linear model with the data in the $I = 0$ channel is surely not fundamental but probably reflects broad resonant enhancements or some other form of attractive dynamics in the isoscalar channel. If there were not additional attractive dynamics in the $I = 0$ channel then the suppressing effect of the t- and u-channel ρ exchanges would be as evident in the $I = 0$ amplitude as they are in the $I = 2$ amplitude.

3.3 The ρ Chiral Lagrangian and Complementarity

The chiral lagrangian is a useful tool for illustrating the complementarity of resonant and nonresonant scattering signals. In particular we consider the chiral lagrangian with the ρ meson incorporated in a chiral invariant fashion. Weinberg[25] showed that chiral invariance requires the conventional $\rho\pi\pi$ interaction,

$$\frac{1}{2} f_{\rho\pi\pi}\ \epsilon_{ijk}\ \rho_i^\mu \pi_j \overleftrightarrow{\partial}_\mu \pi_k, \tag{3.9}$$

to be accompanied by a four pion contact interaction that induces a linear term in

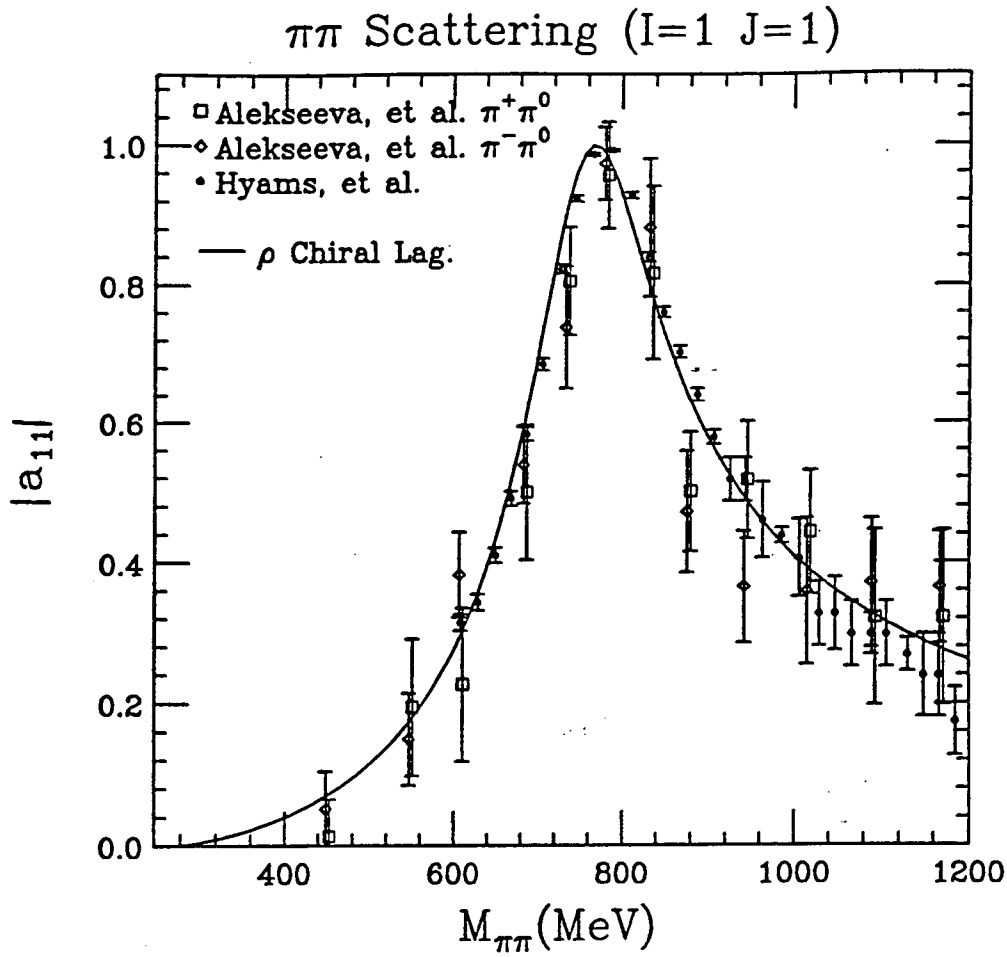

Figure 3.3 The ρ chiral Lagrangian model compared with $\pi\pi$ scattering data for $|a_{11}|$ (W. Kilgore).

s in the $\pi\pi$ scattering amplitude. This term cancels the linear terms induced by the ρ exchanges, so that the low energy theorems are guaranteed. [§]

This chiral lagrangian gives a remarkably good fit of the a_{11} and a_{20} partial waves as shown in figures 3.3 and 3.4 compiled by Kilgore. The quality of the fit at 1.2 GeV is probably fortuitous since the linear terms contributed by the chiral lagrangian should be irrelevant at that scale. The fits show that the chiral lagrangian gives a good parameterization of the QCD data which we can now use to explore the consequences of varying the ρ mass and width. For massless Goldstone bosons w_i the ρ width is given by

[§]It is sometimes argued that the KSRF[27] relation can be obtained by requiring consistency of the s-channel ρ threshold contribution with the low energy theorems. In fact the cross-channel ρ exchanges modify the putative consistency condition to be 3/2 of KSRF. Weinberg's analysis shows that these considerations are spurious and that chiral invariant $\rho\pi\pi$ interactions ensure the low energy theorems regardless of the relationship between m_ρ, $f_{\rho\pi\pi}$, and F_π.

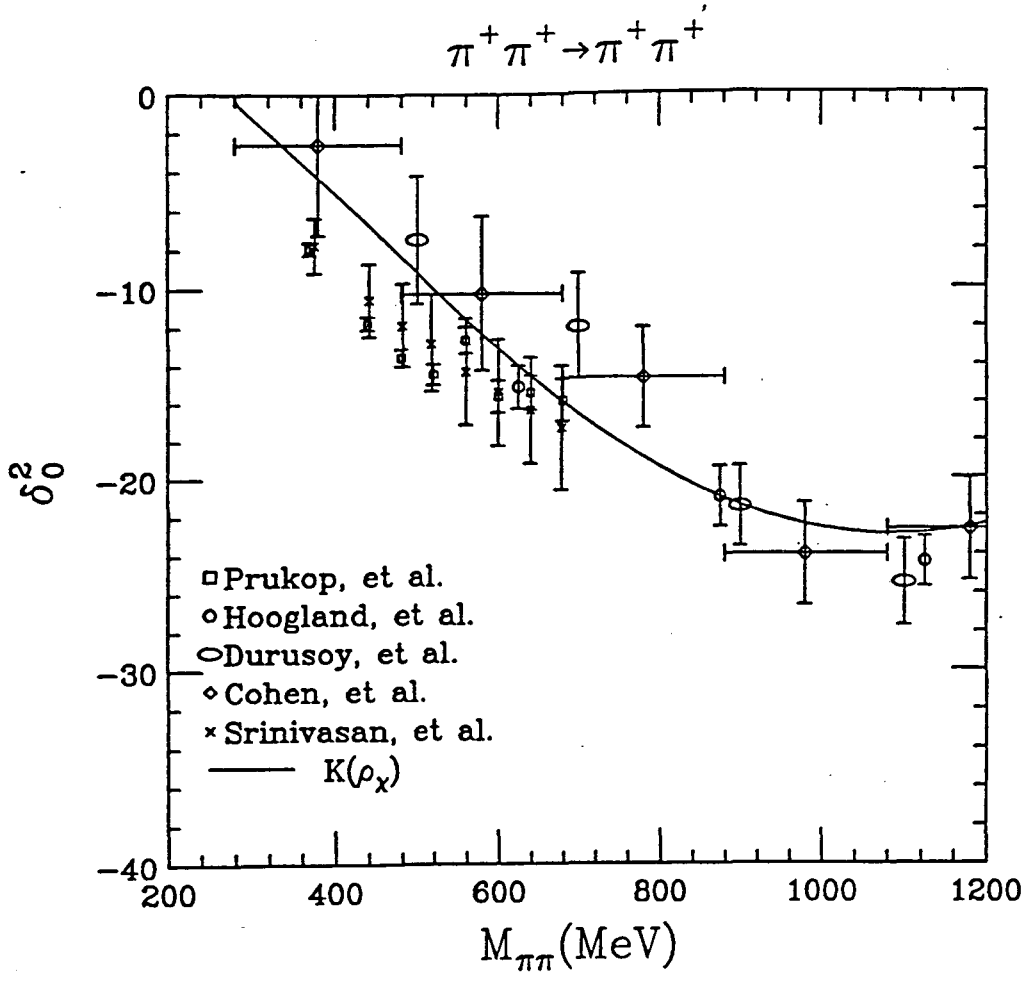

Figure 3.4 The ρ chiral Lagrangian model compared with $\pi\pi$ scattering data for δ_{20} (W.Kilgore).

$$\Gamma_\rho = \frac{f^2_{\rho ww}}{48\pi} m_\rho. \tag{3.10}$$

The lagrangian is completely specified by the Goldstone boson – gauge current coupling v, and the ρ mass and width.

I will consider two examples of "ρ" mesons from minimal, one doublet technicolor, $N_{TC} = 2$ and 4. With the conventional large N_{TC} scaling the mass and width are given in terms of the parameters of the $\rho(770)$ by

$$m_{\rho_{TC}} = \sqrt{\frac{3}{N_{TC}}} \frac{v}{F_\pi} m_\rho \tag{3.11}$$

and

$$\Gamma_{\rho_{TC}} = \frac{3}{N_{TC}} \frac{m_{\rho_{TC}}}{m_\rho} \frac{1}{\beta_\pi^3} \Gamma_\rho. \tag{3.12}$$

where β_π is the pion velocity in the $\rho(770)$ decay. For $N_{TC} = 4$ the mass and width are 1.78 and 0.326 TeV. For $N_{TC} = 2$ they are 2.52 and 0.92 TeV. For larger values of N_{TC} and with the addition of more techniquark doublets the ρ_{TC} becomes lighter and more easily observable. To represent the possibility that the resonances of $\mathcal{L}_5$ may be heavier than the naively anticipated 1 - 3 TeV region I also consider a 4 TeV "ρ" meson with a width of 0.98 TeV determined from the $f_{\rho\pi\pi}$ coupling of the $\rho(770)$.

To ensure unitarity the amplitudes are unitarized by the K-matrix method described above. The width is omitted in the real part of the s-channel pole contributions and the imaginary part (i.e., the width) is then determined from the K-matrix prescription. This K-matrix resonance prescription is essentially equivalent (i.e., precisely equivalent in the s-channel pole approximation) to the conventional broad resonance Breit-Wigner parameterization in which the fixed imaginary part of the denominator, $m\Gamma$, is replaced by $\sqrt{s}\Gamma(\sqrt{s})$. (I thank W. Kilgore for explaining this to me.)

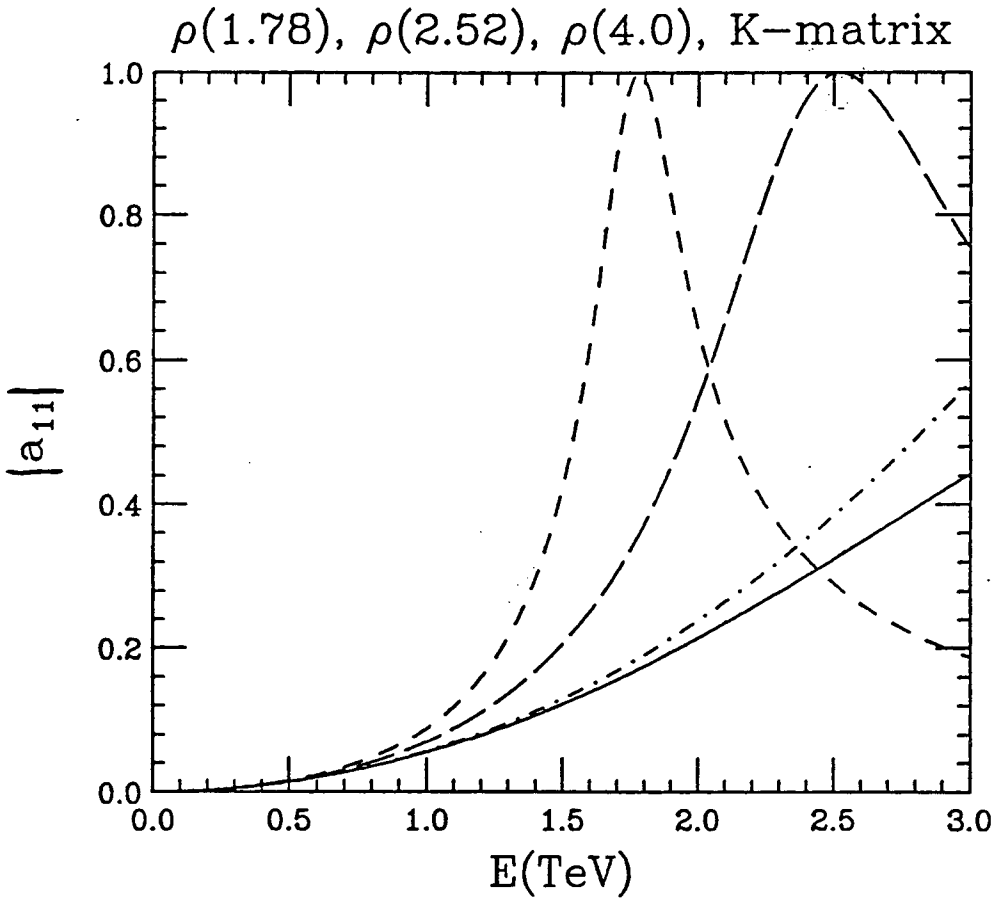

Figure 3.5 $|a_{11}|$ for the "ρ" chiral Lagrangian model with $m_\rho = 1.78$ (dashes), $m_\rho = 2.52$ (long dashes) and $m_\rho = 4.0$ (dot-dash). The nonresonant K-matrix model is represented by the solid line.

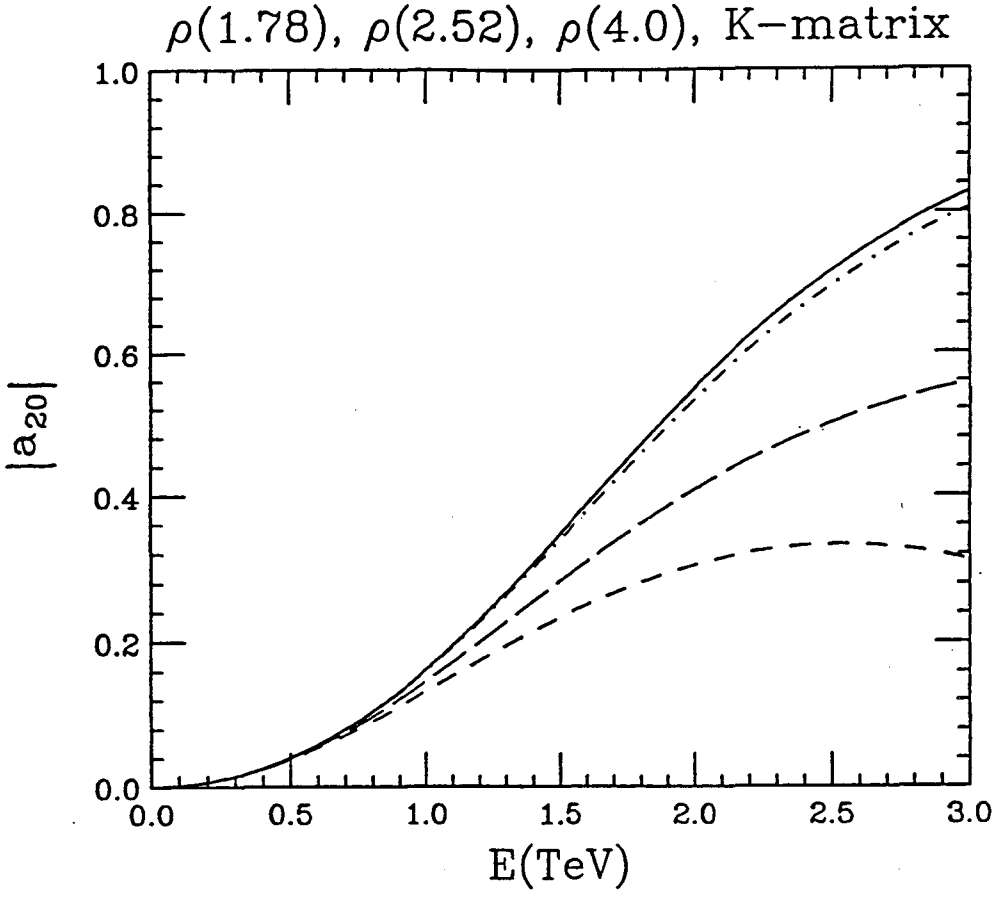

Figure 3.6 $|a_{20}|$ for the "ρ" chiral Lagrangian models and for the nonresonant K-matrix model. Lines are labeled as in Figure 3.5.

The results for the a_{11} and a_{20} amplitudes are shown in figures 3.5 and 3.6 along with the amplitude of the nonresonant K-matrix model discussed in Section 3.2. As expected the amplitudes resemble the nonresonant K-matrix model when the "ρ" mass becomes large. In particular the 4 Tev "ρ" amplitude is very nearly equal to that of the K-matrix model. This is a very general feature, independent of the specific properties of vector meson exchange. It explains the sense in which gradual unitarization models, such as the linear and K-matrix models, are "conservative": they represent the "fail-safe" nonresonant scattering signals that are anticipated if the resonances are unexpectedly heavy. This is the most general meaning of complementarity. A more specific meaning, special to vector meson exchange, is the inverse relationship of the $I = 1$ and $I = 2$ channels that is evident in the figures. The 11 channel provides the largest signal for the lightest resonances while the 20 amplitude

has its largest signal when the resonances are heaviest and therefore exert the least suppression on the amplitude.

3.4 WW Scattering Models from $\pi\pi$ Scattering Data

The $\pi\pi$ scattering data scaled by $v/F_\pi = 2700$ can be used as model of strong W_LW_L scattering, that is relevant to the extent that $\mathcal{L}_5$ resembles $\mathcal{L}_{QCD}$, e.g., as we would expect in a technicolor theory with $N_{TC} = 3$. However there are important pion mass corrections to the simple scaling prescription in the W^+W^+ channel because the pion is actually much heavier than the W boson! That is,

$$\left(\frac{m_\pi}{F_\pi}\right)^2 \gg \left(\frac{M_W}{v}\right)^2. \tag{3.13}$$

Eq. (3.13) implies that the pion mass corrections to the low energy theorems for $\pi\pi$ scattering are much more important (by a factor 20) than the W mass corrections to the W_LW_L low energy theorems. Fortunately the leading pion mass corrections are known and can be included in the scaling prescription. The W mass corrections, $O(M_W/E)$, arising for example as corrections to the ET-EWA approximation, are not known but are small in the energy region we consider.

In the limit $m_\pi = 0$ the $I = 2$, $J = 0$ $\pi\pi$ low energy theorem is

$$a_{20}(\pi^+\pi^+ \to \pi^+\pi^+) = -\frac{s}{32\pi F_\pi^2}. \tag{3.14}$$

The leading $O(m_\pi^2/s)$ correction is determined in QCD by the chiral $SU(3)$ transformation properties of the quark mass terms in $\mathcal{L}_{QCD}$ [20],

$$a_{20}(\pi^+\pi^+ \to \pi^+\pi^+) = -\beta_\pi \frac{s - 2m_\pi^2}{32\pi F_\pi^2}. \tag{3.15}$$

The replacement of s by $s - 2m_\pi^2$ implies a factor 4 suppression in the cross section at threshold relative to the uncorrected amplitude. The kinematical factor β_π is also important in the near threshold region. To account for the suppression near threshold in equation (3.15) we define the scaling model by the prescription[29,6]

$$a_{20,WW}(s_{WW}) = a_{20,\pi\pi}(s_{\pi\pi}) \tag{3.16}$$

where s_{WW} is specified by

$$\beta_W s_{WW} = \beta_\pi \left(\frac{v}{F_\pi}\right)^2 (s_{\pi\pi} - 2m_\pi^2). \tag{3.17}$$

The scaled $\pi\pi$ model is then based on the scattering amplitude that chiral symmetry tells us the pion would have had if it were a true Goldstone boson. This prescription collapses to naive scaling by v/F_π far above threshold, $s_{\pi\pi} \gg 4m_\pi^2$, but near threshold the effect on the signal is large because the $W_L W_L$ luminosity is a steeply falling function of $\tau_{WW} = s_{WW}/s$. The kinematical factors β_W and β_π ensure that the WW and $\pi\pi$ thresholds map into one another but the β_W factor has negligible effect on the magnitude of the signal because the cuts used in Section 5 guarantee the model is only applied far above the WW threshold, at least $\sqrt{s_{WW}} > 0.5$ TeV.

3.5 Criterion for Observability

If there are no prominent resonances or if they are unexpectedly heavier than 1-3 TeV, we will have to rely on structureless continuum signals of strong WW scattering for evidence of the dynamics of $\mathcal{L}_5$. The signals are then excesses of events with no discernible structure. To detect the excess reliably we must understand the background to $\pm 30\%$, a goal consistent with the level at which we can expect to understand the nucleon structure functions and perturbative QCD.[34] Realization of this goal requires an extensive program of "calibration" studies at the SSC and LHC, to measure a variety of jet, lepton, and gauge boson final states in order to tune the structure functions and confirm our understanding of the backgrounds.

The criterion for observability then requires both statistical significance and attention to the "systematic error" due to our imperfect knowledge of the background. Anticipating eventual understanding of the backgrounds to $\pm 30\%$ I will conservatively require that the number of signal events S be at least as large as the number of background events B,

$$S \geq B. \tag{3.18}$$

After some years of experience at the SSC and LHC it may be possible to relax this condition somewhat. For statistical significance I consider both $\sigma^\uparrow$ and $\sigma^\downarrow$, defined as

$$\sigma^\uparrow = S/\sqrt{B} \tag{3.19}$$

$$\sigma^\downarrow = S/\sqrt{S+B}, \tag{3.20}$$

the standard deviations respectively that the background could fluctuate up to give a false signal or that the signal plus background could fluctuate down to the level of the background alone. Minimal criteria for an observable signal are

$$\sigma^\uparrow \gtrsim 5 \tag{3.21}$$

and

$$\sigma^{\downarrow} \gtrsim 3. \tag{3.22}$$

The criterion for $\sigma^{\uparrow}$ is stricter than for $\sigma^{\downarrow}$ since the population of potentially false signals is much greater than the population of true signals.

4. Strong Resonances: the "ρ" Meson

Though there is no theorem forbidding surprises, it seems likely based on our limited experience with strong interaction physics that a strong $\mathcal{L}_5$ would give rise to a prominent two body resonance in the 1 - 3 TeV region, perhaps analogous to the isovector $\rho(770)$. We will deal with the possibility of unpleasant surprises in the subsequent sections when we discuss the continuum strong scattering signals. In this section we will consider the signal for a ρ - like two body resonance in WW scattering. We will model the signals with the chiral lagrangian[25,26] introduced in Section 3.3. Applied to QCD we saw that it gives a very good fit to both the a_{11} and a_{20} partial wave amplitudes (figures 3.3 and 3.4).

There are two important ρ_{TC} production mechanisms: $\bar{q}q$ annihilation[34a] via a virtual W boson and WW fusion.[1] The former is estimated using vector meson dominance of the weak current. The latter in the WZ channel considered below has contributions from both the a_{11} and a_{20} partial waves. The ρ_{TC} decays predominantly to ww, i.e., W_LW_L , just as the $\rho(770)$ decays to $\pi\pi$, so that $f_{\rho ww}$ is determined from the ρ_{TC} width. The large N_{TC} estimates for the mass and width are given in equations (3.11-3.12). I will also consider the signal from the 4 TeV "ρ" resonance with a width of 0.98 TeV introduced in Section 3.3. As in Section 3.3 the amplitudes for both $\bar{q}q$ annihilation and WZ fusion are unitarized by the K-matrix method. The WZ fusion amplitude includes the linear terms from the chiral lagrangian, including the contact interaction induced by the chiral invariant ρ coupling, and the s- and u-channel ρ exchange contributions.

In this and the subsequent sections I consider just the purely leptonic decay modes since the experimental ability to detect the "mixed" decays in which one gauge boson decays hadronically is uncertain — see the study of jet tagging reported in the SDC technical design report.[35] For ρ_{TC} the channel of choice is therefore WZ, which can be cleanly detected in the leptonic final state $l^{\pm}\nu + l^{+}l^{-}$ where l is an electron or muon. The net branching ratio is then 1.4%.

The dominant background, and the only one included in the results given below, is continuum $\bar{q}q$ annihilation to WZ pairs. The calculations use the HMRS structure

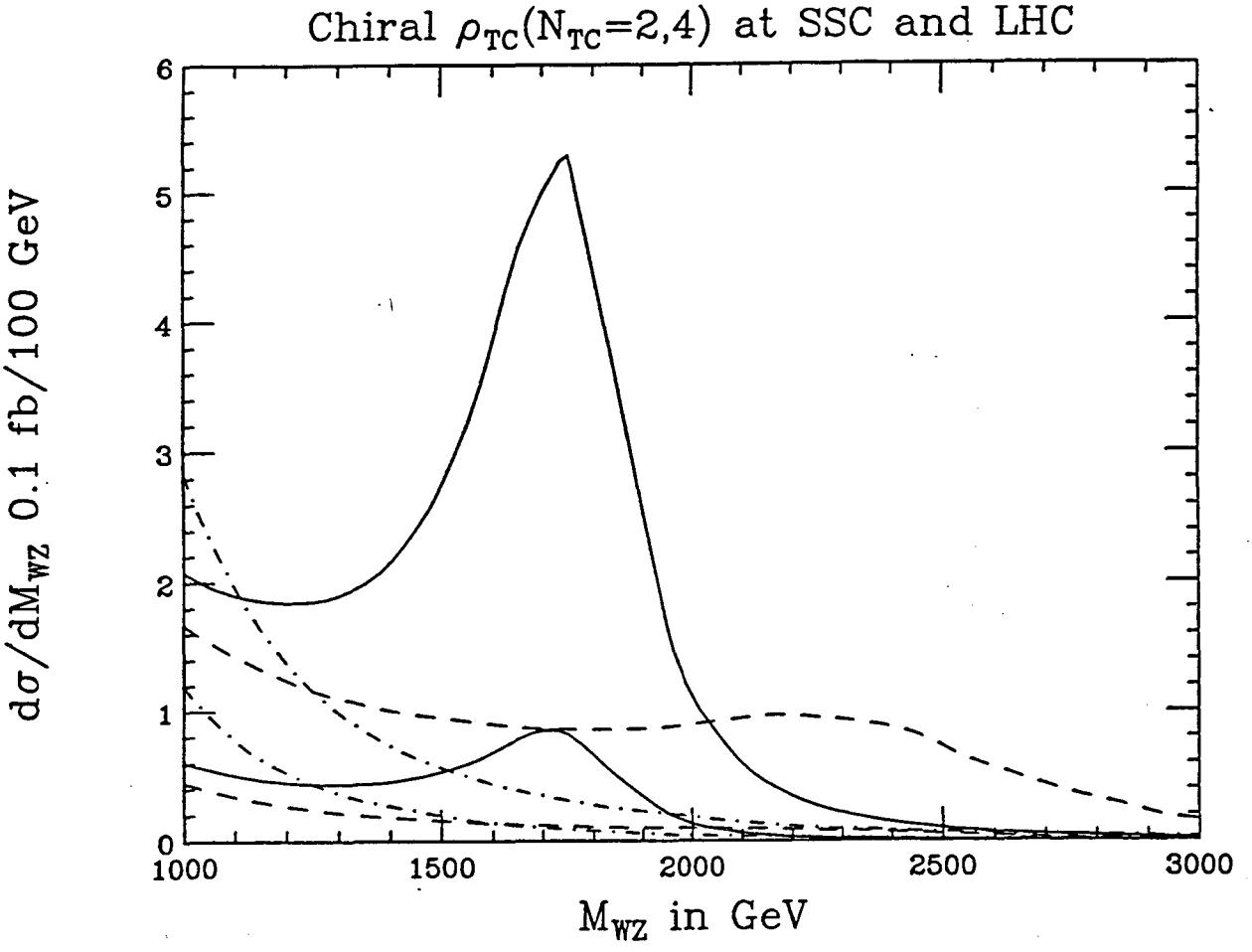

Figure 4.1 $N = 4$ (solid lines) and $N = 2$ (dashed lines) ρ_{TC} signals at the SSC and LHC with branching ratios and cuts specified in the text. The dot-dashed lines indicate the background.

functions. The WZ fusion contribution is computed using the EWA. I have not attempted to fine-tune the cuts for these ρ_{TC} signals since a simple cut in the invariant mass is sufficient to demonstrate the dominance and observability of the signal at the SSC. A more careful treatment of the cuts and the smaller background contributions would be needed to refine the estimates given below of the LHC luminosity requirements and would also improve the SSC signals.

I consider the $N_{TC} = 2$ and 4 ρ_{TC} mesons since they bracket scaled QCD, $N_{TC} = 3$, and because larger values of N_{TC} correspond to smaller masses and bigger signals. The results are summarized in figure 4.1 and table 4.1.

Table 4.1: Yields of $\rho_{TC}^{\pm}$ signal and background events per 10 fb^{-1} at the SSC. Contributions to the signal from WW fusion and $\bar{q}q$ annihilation are shown separately. Statistical significance $\sigma^{\uparrow,\downarrow}$ is defined in Eqs. (3.19-3.20). Cuts are $|y_W| < 1.5$, $|y_Z| < 1.5$, and M_{WZ} as indicated.

$\sqrt{s}$	M_ρ	M_{WZ}	Signal			BKGD	$\sigma^{\uparrow}, \sigma^{\downarrow}$
			WZ	$\overline{Q}Q$	TOT		
40 TeV	1.78	>1.0	19	11	30	9.3	10, 4.8
		>1.4	15	7.7	23	3.3	12, 4.5
	2.52	>1.0	13	4.3	17	9.3	5.7, 3.4
		>1.2	12	3.1	15	5.3	6.3, 3.3
	4.0	>1.0	9.9	2.9	13	9.3	4.2, 2.7
		>1.2	8.1	2.0	10	5.3	4.4, 2.6
16 TeV	1.78	>1.0	1.9	3.5	5.5	3.2	3.0, 1.9
		>1.4	1.4	2.2	3.6	0.9	3.8, 1.7
	2.52	>1.2	0.9	0.8	1.7	1.6	1.4, 0.9
		>1.4	0.7	0.6	1.3	0.9	1.4, 0.9
	4.0	>1.6	0.3	0.2	0.5	0.5	0.7, 0.5

A rapidity cut $|y| < 1.5$ has been applied to the gauge bosons. The tables give the numbers of events per 10 fb^{-1} for various cuts on the diboson invariant mass. The figures plot the signals and backgrounds separately, i.e., the signal is *not* plotted incrementally above the background. The results for the 4 TeV ρ resonance are included in the tables but are not shown in the figure.

Assuming detection efficiencies[35] of 95% for $Z \to l^+l^-$ and 85% for the isolated lepton from $W \to l\nu$, the detection efficiency is 80%. To meet the statistical criterion of Section 3 we must then increase by 10 % the requirements on our theoretical estimates, which are not corrected for detection efficiency, from the values given in Eqs. (3.21 - 3.22) to

$$\sigma^{\uparrow} > 5.5 \tag{4.1}$$

and

$$\sigma^{\downarrow} > 3.3. \tag{4.2}$$

Table 4.1 shows that this criterion is satisfied for both (and indeed all) $\rho_{\rm TC}$ resonances with 10 fb^{-1} at the SSC. with signal:background ratios comfortably greater than 1 as required by Eq. (3.18). For $N_{TC} = 4$ ($M = 1.78$ TeV and $\Gamma = 0.33$ TeV) figure 4.1 shows that the resonance has recognizable structure. For diboson masses

above 1.4 TeV the 23 signal events would be unmistakable above a 3 event background. The $N_{TC} = 2$ signal is more demanding, because of the larger mass, 2.5 TeV, and the much greater width, 0.92 TeV. The signal in this case is nonetheless significant, with 18 signal events over 9 background events for $M_{WZ} > 1$ TeV. The 4 TeV "ρ" does not meet the minimum criterion but comes surprisingly close. With 16 fb^{-1} it would provide a minimally significant signal.

At the LHC the signals are of course smaller and the signal:background *ratios* are also smaller than at the SSC. The cuts for the LHC signals in table 4.1 have been chosen to ensure Eq. (3.18) and to provide statistical significance as near as possible to Eqs. (4.1-4.2). With 160 fb^{-1} the $\rho_{TC}(2.52)$ would just meet the minimum significance criterion, while 33 fb^{-1} would be required to meet the minimum criterion for $\rho_{TC}(1.78)$. For the 4 TeV "ρ" 570 fb^{-1} would be needed for a minimal signal.

Notice that the WW fusion component of the signal depends much more sensitively on the beam energy than the $\bar{q}q$ annihilation contribution to both the signal and the background. This explains most of the larger signal:background ratio at the SSC and causes the $\bar{q}q$ induced fraction of the signal to be larger at the LHC. The $\bar{q}q$ fraction increases the LHC:SSC signal ratio relative to what it would be if the signal were due only to WZ scattering.

Since $N_{TC} = 2$ is the most demanding ρ_{TC} signal these results show that the SSC with 10 fb^{-1} and the LHC with 160 fb^{-1} will be able to discover any techni-rho assuming the conventional large N_{TC} estimates are not badly violated. The luminosity that would be required at the LHC to obtain not just minimally significant signals but equivalent signals to those at the SSC with 10 fb^{-1} are 110, 180, and 330 fb^{-1} for the 1.78, 2.52, and 4.0 TeV "ρ" resonances respectively.

While the 4 TeV "ρ" signal does not quite meet the criterion at the SSC with 10 fb^{-1} , it provides a more than minimal signal in the W^+W^+ scattering channel as expected by complementarity. We could of course imagine even heavier "ρ" resonances with even smaller signals in the WZ channel, but all these would provide robust signals in the W^+W^+ channel as shown in the next section.

5. Strong W^+W^+ Scattering Signals

The W^+W^+ and W^-W^- channels are especially interesting for three reasons:

- They do not have the $\bar{q}q \to WW$ or $gg \to WW$ backgrounds, respectively of order α_W and $\alpha_W\alpha_S$ in amplitude, that are the dominant backgrounds to the strong scattering signals in other gauge boson pair channels. The leading

background to strong W^+W^+ scattering is the order α_W^2 amplitude discussed below.

- The branching ratio for $W^+W^+ \to l^+\nu + l^+\nu$ with $l = e$ or μ is relatively large, $\sim 5\%$, and has a striking experimental signature: two isolated, high p_T, like-sign leptons in an event with no other significant activity (jet or leptonic) in the central region.

- Strong $W^+W^+ + W^-W^-$ scattering complements the strong scattering signals in the other gauge boson pair channels, in that the $W^+W^+ + W^-W^-$ signal is likely to be largest if the resonance signals expected in the other channels are smallest — see Section 3.2.

The W^+W^+ strong scattering signal was first estimated in reference 1 but with no estimate of the backgrounds. There have subsequently been several more detailed studies of signals and backgrounds,[4–6,29] resulting in a powerful set of cuts that greatly enhances the signals with respect to the background. In this section we will consider the signals from the strong scattering models introduced in Section 3: the linear and K-matrix models, scaled $\pi\pi$ scattering data, and the "ρ" chiral lagrangian with the "ρ" parameters considered in the previous section.

5.1 Backgrounds

One would expect the $O(\alpha_S\alpha_W)$ gluon exchange amplitude for $qq \to qqW^+W^+$ to be the dominant background. It was computed and compared to strong scattering signals in reference 29. With correction of a programming error (see erratum[29]) the gluon-exchange cross section of reference 29 is consistent with results reported by Dicus and Vega,[36] who subsequently made the surprising discovery that the electroweak $O(\alpha_W^2)$ background is a few times larger than the contribution of gluon exchange.[37] This conclusion has been confirmed in references 4 - 6.

These order α_W^2 and $\alpha_W\alpha_S$ amplitudes are "irreducible" backgrounds in the sense that they correspond to precisely the same parton scattering process as the strong scattering signal, i.e., $qq \to qqW^+W^+$. In the results presented below I do not consider another set of backgrounds which are more detector dependent and are not irreducible. These are first, $\bar{q}q \to W^+W^- \to l^+\nu l^-\bar{\nu}$ where the l^- charge is mismeasured and second, $\bar{t}t \to W^+W^-$ where the W^+ decays leptonically to l^+ and the W^- decays to $\bar{t}b$ with the b quark decaying semileptonically to a second l^+.

Both of these "non-irreducible" backgrounds have been simulated in the SDC

detector with encouraging results[35], and with the detection capabilities of the SDC both will probably be smaller than the irreducible backgrounds, though a full detector simulation has yet to be done. I am not aware of any similar study for the LHC where the top quark backgrounds are potentially more dangerous. The key to the first background is the tracking capability in a magnetic field to measure the curvature of the lepton track. The key to the second is the isolation of the leptons, since the lepton from b decay will tend to have nearby hadronic fragments from the associated c quark. The isolation cut will be especially powerful for the larger values of p_{Tl}^{MIN} considered below. Topological cuts will also be helpful against the $\bar{t}t$ backgrounds. See also references 4,5, and 38 for other studies of the top quark related background.

The $O(\alpha_W^2)$ background to strong WW scattering is the complete tree approximation amplitude for $qq \to qqWW$ in the standard model with a light Higgs boson, say $m_H \lesssim 100$ GeV. For cuts appropriate to strong WW scattering the $O(\alpha_W^2)$ background amplitude for $qq \to qqW^+W^+$ is independent to a very good approximation of the value of m_H within the range $m_H \lesssim 100$ GeV It consists of W_TW_T (transverse-transverse) and W_TW_L (transverse-longitudinal) pairs with only a negligible quantity of W_LW_L pairs. With the cuts given below the cross section to produce $W_TW_T + W_TW_L$ pairs is essentially independent of m_H even for large values of m_H in the strong scattering domain, $m_H \cong O(1)$ TeV. That $\sigma(W_TW_T + W_TW_L)$ does not depend on m_H is easily understood, since it is the component of $qq \to qqWW$ scattering that occurs via gauge sector interactions rather than by the interactions of $\mathcal{L}_5$ and that would occur at the same level in the unbroken phase of the theory. It is in this sense that it is a "background" to strong W_LW_L scattering.

All WW polarizations, W_TW_T, W_LW_T, and W_LW_L are included in the background calculations reported below. While the W_LW_L contribution to the background is truly negligible, the W_LW_T contribution is not. In particular with cuts like those introduced below that discriminate very effectively against transversely polarized W's, the fraction of W_LW_T events passing the cuts tends to increase relative to W_TW_T and a larger error is committed by neglecting them.

5.2 The Nucleon Q^2 scale

The effective W approximation[23] is an essential ingredient of the strong scattering models. Its validity at large s_{WW} has been verified in many studies. Like the effective photon approximation it is a small angle approximation that neglects the transverse momentum of the recoiling quark that emits the (slightly) virtual W. It is a good approximation at high energy because the neglected transverse momentum (and also

the virtuality of the gauge boson) are of a *fixed* order of magnitude, independent of the scattering energy, given for instance by m_e in the case of the effective photon approximation applied to e^+e^- scattering or by M_W for the EWA applied to qq scattering. Insofar as the EWA is applicable, the quarks in WW fusion are probed by the virtual W's at a Q^2 scale of order M_W^2, and we therefore choose M_W as the scale of the quark distribution functions in the calculations of the ET-EWA model signals,

$$Q^2 = M_W^2. \tag{5.1}$$

The W is then only "slightly" virtual since in the domain of validity we enforce $E_W \gg M_W$.

For the order α_W^2 and $\alpha_W\alpha_S$ amplitude backgrounds a different Q^2 choice is needed because not all the contributions to the background are characterized by a fixed scale of order M_W. The contribution of $\bar{q}q$ annihilation amplitudes, $\bar{q}q \to \bar{q}qWW$ is negligible, and for the remaining t- and u-channel exchange amplitudes we follow the prescription[39,29,6]

$$Q^2 = \frac{1}{2}\,(p_{Tj_1}^2 + p_{Tj_2}^2) + M_W^2, \tag{5.2}$$

where $p_{Tj_{1,2}}$ are the transverse momenta of the final state quark jets. Equation (5.2) has the virtue that for the domain of interest, $p_{TW}^2 \gg M_W^2$, it becomes $Q^2 \cong p_{TW}^2 \cong p_{Tj}^2$ if the W acquires large p_T by recoiling against the emitting quark, while collapsing to $Q^2 \cong O(M_W^2)$, equation (5.1), if the two W's recoil against one another as occurs when WW fusion dominates. It therefore interpolates between the two possible scales at which the nucleons are probed by the virtual W's. (We also use equation (5.2) for the scale of α_S in the gluon exchange amplitude.)

A consistency check of Eqs. (5.1) and (5.2) was performed in reference 39, in which different scale choices were compared for the consistency of the ET-EWA computation of the heavy Higgs boson ($m_H = 1$ TeV) with the full order α_W^2 amplitude calculation of the same signal. Due to a programming error, the results that were attributed to Eq. (5.2) actually corresponded to the choice $Q^2 = \frac{1}{2}\,(p_{TW_1}^2 + p_{TW_2}^2) + M_W^2$. The error does not affect the evidence in support of Eq. (5.1) for the ET-EWA calculations of the signal but may affect the choice of scale for the backgrounds. The question needs more study. In this paper I will use Eqs. (5.1) and (5.2).

The Q^2 scale choice has a significant effect on the signal. For instance, choosing $Q^2 = s_{qq}$ for the ET-EWA signal, as was done in reference 4, results in an order 30% reduction in the signal magnitude.

5.3 Experimental Cuts

In references 1 and 29 the signals were computed using a "theorist's" cut on M_{WW}, the WW invariant mass, that cannot be implemented in the W^+W^+ channel with two neutrinos in the final state. It was supposed that the results would be an upper limit on what could be achieved using measurable variables such as the dilepton mass, m_{ll}, or the transverse dilepton mass, $\sqrt{m_{ll}^2 + p_{T,ll}^2}$. Drawing on the efforts of three groups[4-6] we now have experimentally implementable cuts that are actually much more powerful than the "theorist's" cuts.

The single most effective variable is the lepton transverse momentum, p_{Tl}. The cut $p_{Tl} > p_{Tl}^{MIN}$ is effective for two reasons. First, large p_{Tl} implies large M_{WW} and therefore enhances the signal — which has subprocess amplitude growing with M_{WW} — over the background with subprocess amplitude decreasing as M_{WW} increases. In this respect the p_{Tl} cut replicates the "theorist" cut on M_{WW}. Second, the p_{Tl} variable enhances the longitudinally polarized W bosons of the signal over the predominantly transversely polarized W bosons of the background, and in this respect it surpasses the M_{WW} variable. In fact the p_{Tl} variable is "twice" as good as M_{WW}. For instance, in the case of the linear model signal if we choose p_{TL}^{MIN} and M_{WW}^{MIN} to pass equal numbers of signal events we find that the p_{Tl} cut passes only half as many background events as the M_{WW} cut.

The explanation lies in the decay angular distributions of the W bosons for transversely and longitudinally polarized W's. Defining θ^* as the angle in the W^+ rest frame between the lepton l^+ and the boost axis to the laboratory frame, the distribution for longitudinal W's is

$$\frac{dN}{d\cos\theta^*} = \frac{3}{4}\sin^2\theta^* \tag{5.3}$$

while for transverse W's it is

$$\frac{dN}{d\cos\theta^*} = \frac{3}{8}(1+\cos^2\theta^*). \tag{5.4}$$

The distribution peaks at 90^0 for W_L while for W_T it peaks in the forward and backward directions.

Since we always impose "hard" cuts that ensure $E_W \gg M_W$ (essential for the validity of the ET-EWA based models and also useful against the backgrounds), most of the leptons born of W_L will be "hard" and move in the same direction as the parent W_L in the laboratory, while only half the leptons born of W_T will have these properties. The other half, that decay opposite to the W line of flight, will be "soft", i.e., have only a small fraction of the parent W_T's energy, and their direction of motion will be

Table 5.1: Cumulative effect of cuts on linear model signal and background for W^+W^+ only at the SSC. Entries are events per 10 fb^{-1}.

Cut	Signal (++) Linear Model	Background (++) $O(\alpha_w^2)$	$O(\alpha_w\alpha_s)$	Total
$\|y_\ell\| < 2$	71	389	171	560
$p_{T\ell} > 0.1$ TeV	44	38	11	49
$\cos\varphi_{\ell\ell} < -0.975$	32	6.7	2.4	9.1
CJV	27	2.3	0.18	2.4

weakly correlated with the parent boson's. This makes the $p_{Tl} > p_T^{MIN}$ cut highly effective against the W_TW_T background and, to a lesser extent, against the W_TW_L background.

A second useful variable, introduced in reference 5, favors longitudinal over transverse gauge bosons for essentially the same reason. It is

$$\cos\phi_{ll} \equiv \hat{p}_{Tl_1} \cdot \hat{p}_{Tl_2} \tag{5.5}$$

the cosine of the angle between the two charged leptons in the transverse momentum plane. For the W_LW_L events the $dN/d\cos\phi_{ll}$ distribution is strongly peaked at $\cos\phi_{ll} = -1$, since the hard leptons "remember" the nearly back-to-back transverse momenta of their parent bosons. For the W_TW_T background events there is a backward peak corresponding to the roughly 25% of the events that contain two hard charged leptons, while the remaining $\sim$ 75% are distributed fairly uniformly. We favor a harder cut on $\cos\phi_{ll}$ than was used in reference 5. The difference may reflect the different signals considered: strong scattering models here versus Higgs boson exchange in reference 5.

The power of these cuts is evident in table 5.1, which shows just the positive W^+W^+ signal and irreducible $O(\alpha_W^2)$ and $O(\alpha_W\alpha_S)$ backgrounds for the linear model (with HMRS structure functions). With only the lepton rapidity cut, $|y_l| < 2$, the background dominates the signal by an order of magnitude, with 71 signal events and 560 background events for 10 fb^{-1} .[¶] The lepton transverse momentum cut $p_{Tl} > 100$ GeV then reduces the background by an order of magnitude, to 49 events,

[¶]Little is gained by increasing the lepton rapidity cut beyond 2, since the background tends to be more forward peaked than the signal. The choice $|y_l| < 2$ is not an experimentally dictated compromise but is consistent with our overall strategy of signal optimization.

while reducing the signal by only 16% to 44 events, already larger than the background. The cut on $\cos\phi_{ll}$ then reduces the background by another factor of 5 to 9 events while retaining 32 signal events, already an extremely clean and significant signal.

The final entry in table 5.1 shows the additional effect of the central jet veto (CJV) proposed by Barger et al.[4], which rejects events with a jet in the central region, $|y_j| < 2.5$, with transverse momentum $p_{Tj} > 60$ GeV. It reduces the background by another factor of 4 and is especially effective against the gluon exchange component of the background which it reduces to insignificance, while diminishing the signal by only about 15%. Unlike forward jet tagging which may be experimentally difficult and has an uncertain and possibly low efficiency,[35] the central jet veto is easy to implement. Like the other cuts the CJV exploits the polarization of signal and background: the longitudinal virtual W's associated with the signal tend to be emitted colinearly at high energy so that the recoil jets are at larger rapidity with smaller p_{Tj}. But the transverse W's cannot be emitted in the forward direction because of angular momentum and (approximate) chirality conservation, therefore the jets recoil at smaller rapidity and larger p_{Tj}.

It is not possible to evaluate the signal efficiency for the CJV using the ET-EWA, since the latter is a small angle approximation that neglects the transverse momentum of the quarks. I have computed the signal efficiency by considering the $m_H \to \infty$ limit of the $O(\alpha_W^2)$ standard model amplitude. With a cutoff at $\sqrt{32\pi v^2} = 2.5$ TeV, it is equivalent to the linear model Eq. (3.11). While the results vary slightly with p_{Tl} and $\cos\phi_{ll}$, the signal and background efficiencies are approximately 85% and 25% respectively at the SSC and 80% and 18% at the LHC. (In the results reported below I have included the slight variation of the CJV efficiency as a function of p_{Tl} and $\cos\phi_{ll}$.) This calculation of the CJV signal efficiency is reliable *to lowest order in QCD* but may overestimate the actual signal efficiency because of high order corrections including gluon radiation.

With the central jet veto the net effect of the cuts is to reduce the background by a factor of 230 while the signal is reduced by only a factor of 2! Without the CJV the result is still very impressive: a factor 60 reduction of the background and less than a factor 2 signal reduction. Since the real CJV signal efficiency may be lower because of gluon radiation, the real net efficiencies lie somewhere between the results with and without the CJV. I will therefore present the results for the various models with and without the CJV.

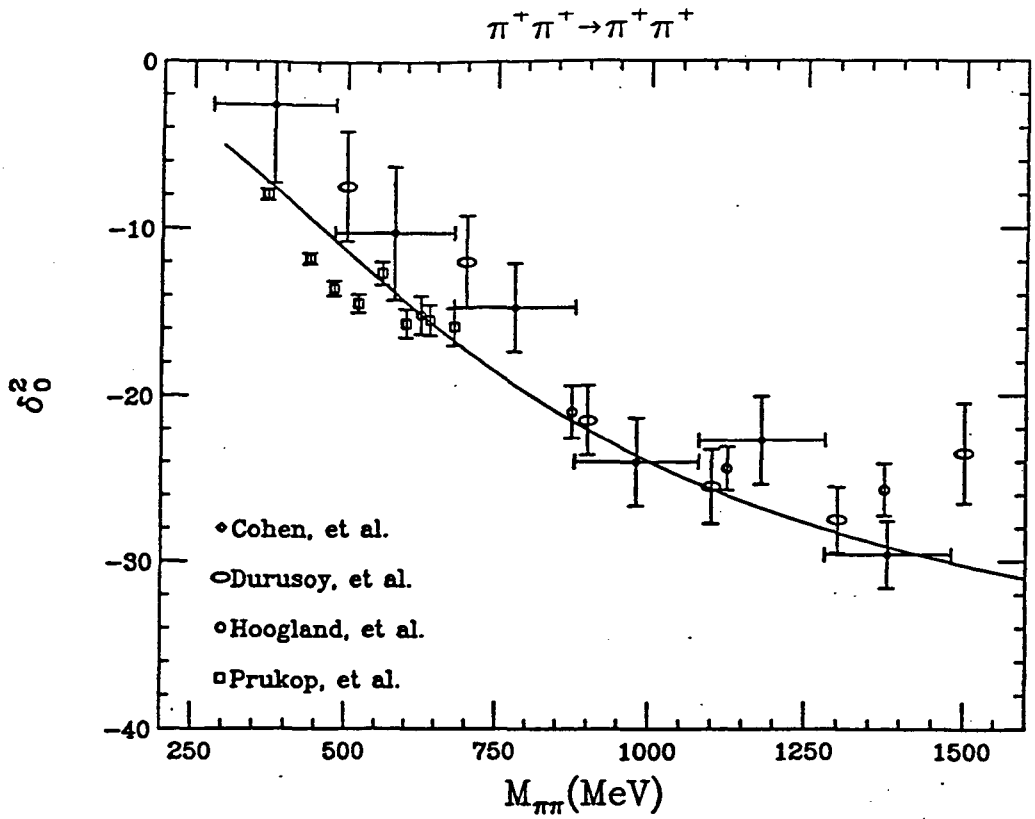

Figure 5.1 $\pi^+\pi^+$ scattering data with the fit of reference 4.

5.4 Results

In this section I will present the results from the linear and K-matrix models, Eqs. (3.11 - 3.12), and from scaled $\pi^+\pi^+$ scattering data using the scaling prescription Eqs. (3.16 - 3.17). Signals for "ρ" chiral Lagrangian will be presented in Section 5.5. A compilation of the $\pi\pi$ scattering data (by M.Berger) is shown in figure 5.1. We consider two fits. Model B, taken from Barger et al.,[4] is represented by the solid line in the figure. Since it underestimates the magnitude of the amplitude at low energy relative to the highest statistics data points, from the experiment of Prukop et al., [40] we consider another fit, model A, based directly on the Prukop et al. data below 600 MeV and matching smoothly to the Barger et al, fit above. The four models presented in this section were studied previously by M. Berger and me,[6] though with EHLQ rather than HMRSB structure functions, without applying the CJV, and only for 40 TeV.

The detection efficiency for an isolated central lepton is assumed to be 85% for the SDC detector,[35] based in part on CDF experience. Therefore the detection efficiency for W^+W^+ pairs decaying to electrons and/or muons is $\simeq$ 70%. To achieve the minimum significance criterion of Eqs. (3.21 - 3.22) for the detected events we scale the minimum criterion for the uncorrected cross sections upward by $1/0.85 = 1.18$,

Table 5.2: Linear model signal and background for $W^+W^+ + W^-W^-$ at SSC and LHC with and without central jet veto. Yields are in events per 10 fb^{-1}. Cuts are $|y_\ell| < 2$, $\cos\varphi_{\ell\ell} < -0.975$, and $p_{T\ell}$ as shown.

		Without CJV				With CJV			
$\sqrt{s}$	$p_{T\ell}$	Bkgd	Linear Model			Bkgd	Linear Model		
TeV	TeV	events	events	$\sigma^\uparrow$	$\sigma^\downarrow$	events	events	$\sigma^\uparrow$	$\sigma^\downarrow$
40	>0.1	14	44	12	5.8	3.8	36	19	5.7
	>0.2	3.5	30	16	5.2	0.8	26	29	5.0
	>0.3	1.2	19	17	4.2	0.3	16	29	4.0
16	>0.1	2.9	4.4	2.6	1.6	0.55	3.6	4.9	1.8
	>0.2	0.5	2.5	3.5	1.4	0.09	2.1	6.9	1.4
	>0.3	0.13	1.3	3.6	1.1	0.03	1.1	6.7	1.0

to

$$\sigma^\uparrow \gtrsim 6 \tag{5.6}$$

and

$$\sigma^\downarrow \gtrsim 3.5. \tag{5.7}$$

The results for the linear, K-matrix, and $\pi\pi$ scattering models are shown in tables 5.2 - 5.5. The cuts have been chosen to maximize $\sigma^\uparrow$ before application of the CJV. The tables give the numbers of signal and background events per 10 fb^{-1} and the values of $\sigma^{\uparrow,\downarrow}$ at both the SSC and LHC. For the linear and K-matrix models harder cuts on p_{Tl} and $\cos\phi_{ll}$ are used than for the $\pi^+\pi^+$ scattering

Table 5.3: K-matrix model signal and background as in Table 5.2.

		Without CJV				With CJV			
$\sqrt{s}$	$p_{T\ell}$	Bkgd	K-matrix			Bkgd	K-matrix		
TeV	TeV	events	events	$\sigma^\uparrow$	$\sigma^\downarrow$	events	events	$\sigma^\uparrow$	$\sigma^\downarrow$
40	>0.1	14	35	9.4	5.0	3.8	29	15	5.1
	>0.2	3.5	23	12	4.4	0.8	20	23	4.4
	>0.3	1.2	13	12	3.5	0.3	12	22	3.4
16	>0.1	2.9	3.9	2.3	1.5	0.55	3.2	4.3	1.7
	>0.2	0.5	2.0	2.8	1.3	0.09	1.7	5.5	1.3
	>0.3	0.13	1.0	2.7	0.9	0.03	0.85	4.9	0.9

Table 5.4: Pion scattering model A as in Table 5.2 except $\cos\varphi_{\ell\ell} < -0.90$.

		Without CJV				With CJV			
$\sqrt{s}$	$p_{T\ell}$	Bkgd		$(\pi\pi)_A$		Bkgd		$(\pi\pi)_A$	
TeV	TeV	events	events	$\sigma^\uparrow$	$\sigma^\downarrow$	events	events	$\sigma^\uparrow$	$\sigma^\downarrow$
40	>0.1	26	63	12	6.7	6.5	52	21	6.8
	>0.15	12	38	11	5.4	3.0	33	19	5.5
	>0.2	6	23	9	4.2	1.5	20	16	4.3
16	>0.1	5.4	10.5	4.5	2.6	1.0	8.2	8.2	2.7
	>0.15	2.0	5.7	4.1	2.1	0.34	4.6	7.8	2.1
	>0.2	0.85	2.9	3.1	1.5	0.12	2.3	6.8	1.5

scaled models, since the latter have proportionately more signal at low energy. The SSC signals easily satisfy Eqs. (5.6 -5.7) and in some cases are quite spectacular in the dominance of the signal over the background. The largest SSC signals occur for the linear model, table 5.2, where for instance with the CJV and $p_{Tl} > 0.3$ TeV the signal is *two* orders of magnitude large than the signal. At such large values of p_{Tl} the top quark associated background will also be extremely small, since the efficacy of the lepton isolation cut increases with increasing p_{Tl} while $d\sigma(\bar{t}t)/dp_{Tl}$ decreases. The most challenging model is the $\pi\pi$ data model B, table 5.5. At the SSC the 10 fb^{-1} signal for model B also passes the minimum criterion with or without the central jet veto.

The LHC signals are of course smaller and have smaller signal:background ratios than the SSC. However the difference in the signal:background ratio is less dramatic

Table 5.5: Pion scattering model B as in Table 5.2 except $\cos\varphi_{\ell\ell} < -0.90$.

$\sqrt{s}$	$p_{T\ell}$	Bkgd		$(\pi\pi)_B$		Bkgd		$(\pi\pi)_B$	
TeV	TeV	events	events	$\sigma^\uparrow$	$\sigma^\downarrow$	events	events	$\sigma^\uparrow$	$\sigma^\downarrow$
40	>0.1	26	33	6.5	4.3	6.5	27	11	4.7
	>0.15	12	21	6.3	3.7	3	18	10	3.9
	>0.2	6	14	5.7	3.1	1.5	12	10	3.3
16	>0.1	5.4	5.0	2.2	1.6	1.0	3.9	3.9	1.8
	>0.15	2.0	2.7	2.0	1.3	0.34	2.2	3.7	1.4
	>0.2	0.85	1.5	1.6	1.0	0.12	1.2	3.5	1.0

than in other channels, such as the ZZ channel considered in the Section 6. The reason is easy to understand. In the ZZ channel the dominant backgrounds are from $\bar{q}q \to ZZ$ and $gg \to ZZ$, with two body phase space which decreases more slowly with energy than does the WW scattering process, $qq \to qqWW \to qqZZ$, with four body phase space. In the W^+W^+ channel both the signal and the background have four body final states, $qq \to qqWW$, and therefore the signal and background scale more nearly alike with beam energy. It should be noted however that the top quark related backgrounds, that are not included in the tables, may be a bigger problem proportionately at the LHC because the additional particles from overlapping events might obscure the isolation of the W decay leptons. Indeed, all aspects of the W^+W^+ signal will have to be examined in the 10^{34} cm^{-2} sec^{-1} luminosity environment.

At the LHC the most significant signal occurs for $\pi\pi$ model A, because that model has a particularly large cross section at low WW energy, reflecting the Prukop et al.[40] "bulge." As for the SSC the $\pi\pi$ model B provides the smallest signal, though at the LHC it is not much smaller than the K-matrix model. The ρ chiral Lagrangian fit, figure 3.4, suggests that model B is probably more plausible than model A.

We may ask what integrated luminosity would enable the LHC signals to meet the minimum criterion Eqs. (5.6 - 5.7). Excluding $\pi\pi$ scattering model A (for which 20 fb^{-1} suffices) the required luminosity varies between 75 fb^{-1} (for model B without CJV) to 40 fb^{-1} (for the linear model with CJV). ‖ These minimal LHC signals are of course less significant than the SSC signals obtained with 10 fb^{-1} . We may ask at what luminosity the LHC would yield a comparable signal, say for the linear model, to the SSC signal with 10 fb^{-1} . The answer to that question for strong scattering into the ZZ final state is 350 fb^{-1} as presented in Section 6. For the W^+W^+ signal a smaller increase is needed, since the energy dependence of the four body final state background more nearly resembles that of the signal. The SSC signal for the linear model with $p_{Tl} > 0.2$ TeV is 30 signal events over 3.5 background events with 10 fb^{-1} . To achieve the same signal:background ratio at the LHC we must raise the p_{Tl} cut to $p_{Tl} > 0.275$ TeV, yielding 1.5 signal and 0.18 background events. A factor 20 increase in luminosity to 200 fb^{-1} then yields 30 signal and 3.6 background events, virtually identical to the 10 fb^{-1} SSC signal.

5.5 Complementarity and the "ρ" Chiral Lagrangian

We have seen in figure 3.4 that the ρ chiral Lagrangian fits the $\pi\pi$ scattering

‖In reaching this conclusion we do not allow $p_{Tl} < 100$ GeV lest we include a significant number of events with $M_{WW} < 500$ GeV for which the ET-EWA breaks down.

Table 5.6: Signals and backgrounds in events per 10 fb^{-1} at the SSC for the "ρ" chiral Lagrangian model. The cuts are specified by the minimum allowed value of $p_{T\ell}$ and the maximum allowed value of $\cos\varphi_{\ell\ell}$

M_ρ	CUT $p_{T\ell}$ / $\cos\varphi_{\ell\ell}$	Without CJV SIG	BKGD	$\sigma^\uparrow, \sigma^\downarrow$	With CJV SIG	BKGD	$\sigma^\uparrow, \sigma^\downarrow$
1.78	0.1 / −0.925	22	23	4.6, 3.3	18	5.7	7.6, 3.7
2.52	0.1 / −0.925	31	23	6.4, 4.2	25	5.7	11, 4.5
	0.15 / −0.90	23	12	6.8, 3.9	20	2.9	12, 4.1
4.0	0.1 / −0.95	40	19	9.1, 5.2	33	4.8	15, 5.3
	0.2 / −0.975	22	3.5	11, 4.3	20	0.9	21, 4.4

data in the $I = 2$ channel to the surprisingly large energy scale of 1.2 GeV. In this section we present the predictions of the model for W^+W^+ scattering using the "ρ" parameters considered in section 4 for the WZ resonance production channel. From figures 4.5 and 4.6 we anticipate that the parameters that gave the smallest signals in the WZ channel will give the largest signals in W^+W^+ scattering. We also expect that the 4 TeV "ρ" model will give a very similar result to that of the nonresonant K-matrix model presented in Section 5.4. As in Sections 3 and 4 we unitarize the amplitudes by the K-matrix prescription.

The results are presented in tables 5.6 and 5.7 for the SSC and LHC respectively. In table 5.6 we see that for the SSC with 10 fb^{-1} the 4 TeV "ρ" model provides a very striking signal that is indeed similar to the K-matrix model signals in table 5.3. The signal for the $N_{TC} = 2$ $\rho_{TC}(2.52)$ is significant even without the central jet veto. The most difficult signal, corresponding to the $N_{TC} = 4$ $\rho_{TC}(1.78)$, meets the minimum criterion with the CJV but without the CJV would require 17 fb^{-1} integrated

Table 5.7: Signals and backgrounds in events per 10 fb^{-1} at the LHC for the "ρ" chiral Lagrangian model. Cuts are specified as in Table 5.6. $\mathcal{L}_{\rm MIN}$ and $\mathcal{L}_{\rm EQ}$ are defined in the text and are given in fb^{-1}.

M_ρ	CUT $p_{T\ell}$, $\cos\varphi_{\ell\ell}$	Without CJV SIG	BKGD	$\sigma^\uparrow, \sigma^\downarrow$	With CJV SIG	BKGD	$\sigma^\uparrow, \sigma^\downarrow$
1.78	0.15, −0.95 (No CJV)	1.8	1.5	1.5, 1.0	2.7	1.0	2.7, 1.4
	0.1, −0.9 (CJV)	$\mathcal{L}_{\rm MIN} = 170$			$\mathcal{L}_{\rm MIN} = 60$		
		$\mathcal{L}_{\rm EQ} = 100$			$\mathcal{L}_{\rm EQ} = 80$		
2.52	same	2.4	1.5	2.0, 1.2	3.3	1.0	3.4, 1.6
		$\mathcal{L}_{\rm MIN} = 95$			$\mathcal{L}_{\rm MIN} = 50$		
		$\mathcal{L}_{\rm EQ} = 110$			$\mathcal{L}_{\rm EQ} = 110$		
4.0	same	3.3	1.5	2.7, 1.5	4.3	1.0	4.3, 1.9
		$\mathcal{L}_{\rm MIN} = 55$			$\mathcal{L}_{\rm MIN} = 35$		
		$\mathcal{L}_{\rm EQ} = 120$			$\mathcal{L}_{\rm EQ} = 200$		

luminosity. It of course provides the biggest signal in the WZ channel, far in excess of the minimum criterion.

The analogous signals for 10 fb^{-1} at the LHC are shown in table 5.7. Also shown in each case are $\mathcal{L}_{MIN}$, the integrated luminosity that would be required to meet the minimum significance criterion, and $\mathcal{L}_{EQ}$, the luminosity to obtain an equivalent signal to that of the SSC with 10 fb^{-1} .

The complementarity of the SSC signals is summarized in table 5.8 which shows that for each "ρ" mass there is an observable signal at the SSC with 10 fb^{-1} even if

Table 5.8: Summary of the complementary signals in the $W^\pm Z$ and $W^+W^+ + W^-W^-$ channels (without CJV) at the SSC in events per 10 fb^{-1}.

M_ρ	$W^\pm Z$ SIG	BKGD	$\sigma^\uparrow, \sigma^\downarrow$	$W^+W^+ + W^-W^-$ SIG	BKGD	$\sigma^\uparrow, \sigma^\downarrow$
1.78	30	9	10, 4.8	22	23	4.6, 3.3
2.52	18	9	5.7, 3.4	23	12	6.8, 3.9
4.0	13	9	4.2, 2.7	40	19	9.1, 5.2

Table 5.9: Summary of luminosity requirement at the LHC ($\mathcal{L}_{\rm MIN}$) to meet the minimum significance criterion for the $W^{\pm}Z$ and $W^+W^+ + W^-W^-$ channels (without CJV).

M_ρ	$\mathcal{L}_{\rm MIN}(fb^{-1})$	
(TeV)	$W^{\pm}Z$	$W^+W^+ + W^-W^-$
1.78	33	170
2.52	160	95
4.0	570	55

we conservatively do not use the central jet veto. The $\rho_{TC}(2.52)$ provides an observable signal in both channels as does the $\rho_{TC}(1.78)$ if we do use the CJV. Without using the CJV all three models would be observable in both channels if the SSC luminosity is increased to only 17 fb^{-1} .

The analogous LHC luminosity requirements are summarized in table 5.9, which gives the luminosity for a minimal signal for each "ρ" mass in both the WZ and W^+W^+ channels. We see that 100 fb^{-1} would guarantee for each model a signal that would be observable above the irreducible backgrounds in one (but never both) of the two channels. However "non-irreducible" backgrounds that are known to be manageable at 10^{33} cm^{-2} sec^{-1} may pose problems at higher luminosity. No firm conclusion can be drawn until these issues have been carefully studied in the relevant channels.

6. Strong Scattering in the ZZ Final State

If $\mathcal{L}_5$ is strongly interacting and if a single symmetry breaking condensate gives mass to both the weak gauge bosons and to the top quark, then there will in general be *two* strong scattering mechanisms for ZZ pair production. They are WW fusion, $W^+W^- \to ZZ$, as discussed in Section 2.4, and gluon-gluon fusion, $gg \to ZZ$, via a top quark loop.[7] As reviewed in Section 2, the WW fusion process probes the mass scale of the quanta which generate the condensate that gives mass to W and Z. The gg fusion process via a virtual $\bar{t}t$ loop probes in a similar way the mass scale of the quanta which make the condensate that generates the t quark mass. If only one condensate does both jobs and if $\mathcal{L}_5$ is strong so that the mass scale of the associated quanta is above 1 TeV, the gg fusion contribution significantly enhances the strong scattering signal in the ZZ final state.** In effect we are generalizing the two

**Here as elsewhere we are assuming $\mathcal{L}_5$ has no light quanta. If there are light PGB's they can induce an additional large contribution to $gg \to ZZ$.[41]

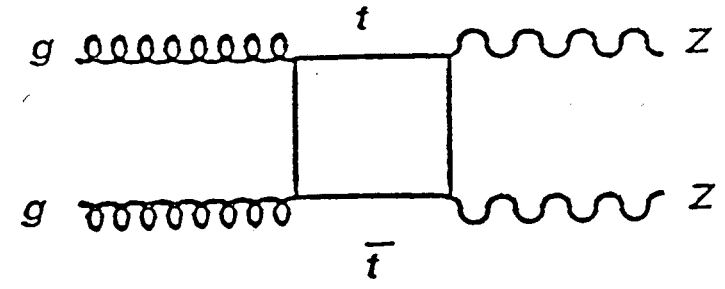

(a)

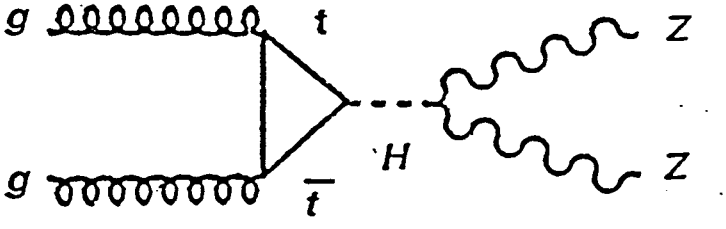

(b)

Figure 6.1 Box and triangle diagrams for $gg \to ZZ$.

principal Higgs boson production mechanisms, $gg \to H$,[42] and $WW \to H$,[43] to the case of dynamical symmetry breaking by a strong $\mathcal{L}_5$.

It is possible to use the WW and gg induced processes to probe separately the mechanisms of gauge boson and matter field mass generation, that do not necessarily arise from the same symmetry breaking condensates. Condensates that contribute to the W and Z masses need not contribute at all to fermion masses, while any condensate that generates quark and lepton masses must contribute to but not necessarily dominate the W and Z masses. Model builders have rarely exercised the option but that is no assurance that nature has not. It will be possible to probe for multiple condensates in second generation experiments with the SSC operating above its initial design luminosity.

6.1 The "Linear Model" for $gg \to ZZ$

In analogy to the enforcement of unitarity in strong WW scattering by the Higgs mechanism, the contribution of gg fusion to the strong scattering signal is best understood by first considering the process $\bar{t}t \to Z_L Z_L$, that contributes to the imaginary part of the $gg \to Z_L Z_L$ amplitude by the unitarity relation

$$Im\ \mathcal{M}(gg \to Z_L Z_L) = -\frac{1}{2}\sum_n \mathcal{M}^*(n \to gg)\mathcal{M}(n \to Z_L Z_L). \qquad (6.1)$$

The contribution to equation 6.1 from the $n = \bar{t}t$ intermediate state can be visualized by cutting through the top quark loops in figure 6.1, which shows the leading diagrams for $gg \to ZZ$ in the Weinberg-Salam Higgs boson model. Omitting symmetry breaking sector interactions, the chirality-flip (equal helicity) amplitude $\bar{t}_+ t_+ \to Z_L Z_L$ also has bad high energy behavior (t_+ denotes a top quark with positive helicity),

$$\mathcal{M}(\bar{t}_+ t_+ \to Z_L Z_L) = \frac{\sqrt{s} m_t}{v^2}. \tag{6.2}$$

Compared to equation (2.36) for $WW \to ZZ$, this bad high energy behavior is less evil by a factor $\sqrt{s}$, a result of the factor m_t needed to flip the chirality.[44] In analogy to equation (2.48) good high energy behavior is restored in the minimal Higgs boson model by adding the s-channel Higgs boson exchange amplitude to equation (6.2),

$$\mathcal{M}(\bar{t}_+ t_+ \to H \to Z_L Z_L) = -\frac{\sqrt{s} m_t}{v^2} \frac{s}{s - m_H^2}. \tag{6.3}$$

More generally the $\sqrt{s}$ growth is cut off by s-channel exchange of whatever the quanta are in the symmetry breaking sector which form the vacuum condensate that generates the top quark mass. If those quanta are very heavy the $\bar{t}t \to Z_L Z_L$ amplitude grows to a larger value before being cut off.

The simplicity of the analogy is complicated by the fact that in gg fusion the top quarks are virtual. In particular the $\sqrt{s}$ bad high energy behavior of equation (6.2) does not induce bad high energy behavior in $\mathcal{M}(gg \to Z_L Z_L)$ because the factor $\mathcal{M}(gg \to \bar{t}t)$ in the unitarity relation equation (6.1) is proportional to $m_t/\sqrt{s}$ in the chirality-flip channel. Glover and van der Bij[45] find by explicit calculation of the box diagrams a contribution to $\mathcal{M}(gg \to Z_L Z_L)$ proportional to $m_t^2 \cdot \log^2 s$, which is engendered by equation (6.2) and is cancelled for $s > m_H^2$ by an opposite contribution from the triangle amplitude figure 6.1b, just as equation (6.3) cancels equation (6.2). In general then $\sigma(gg \to ZZ)$ is sensitive to the masses of the quanta that form the m_t generating vacuum condensate, with a larger high energy cross section if the masses of the m_t generating quanta are very heavy.

Suppose a single condensate generates gauge boson and matter field masses. For the $WW \to ZZ$ strong scattering amplitude we will adopt the linear model, Eq. (3.7). To represent $gg \to Z_L Z_L$ we similarly cut off the $\sqrt{s}$ growth of equation (6.2) at $s_0 = 16\pi v^2 = (1.75\text{TeV})^2$, beyond which the factor $\sqrt{s}$ is replaced by a constant factor $\sqrt{s_0}$. The effect on $gg \to ZZ$ is to retain only the box graphs with the term[††] engendered by equation (6.2) multiplied by a factor $\sqrt{s_0/s}$ for $s > s_0$. If M_W and m_t

[††]The relevant term, with both real and imaginary parts, is $C(s)$ in Eq. (3.24) of ref. 45.

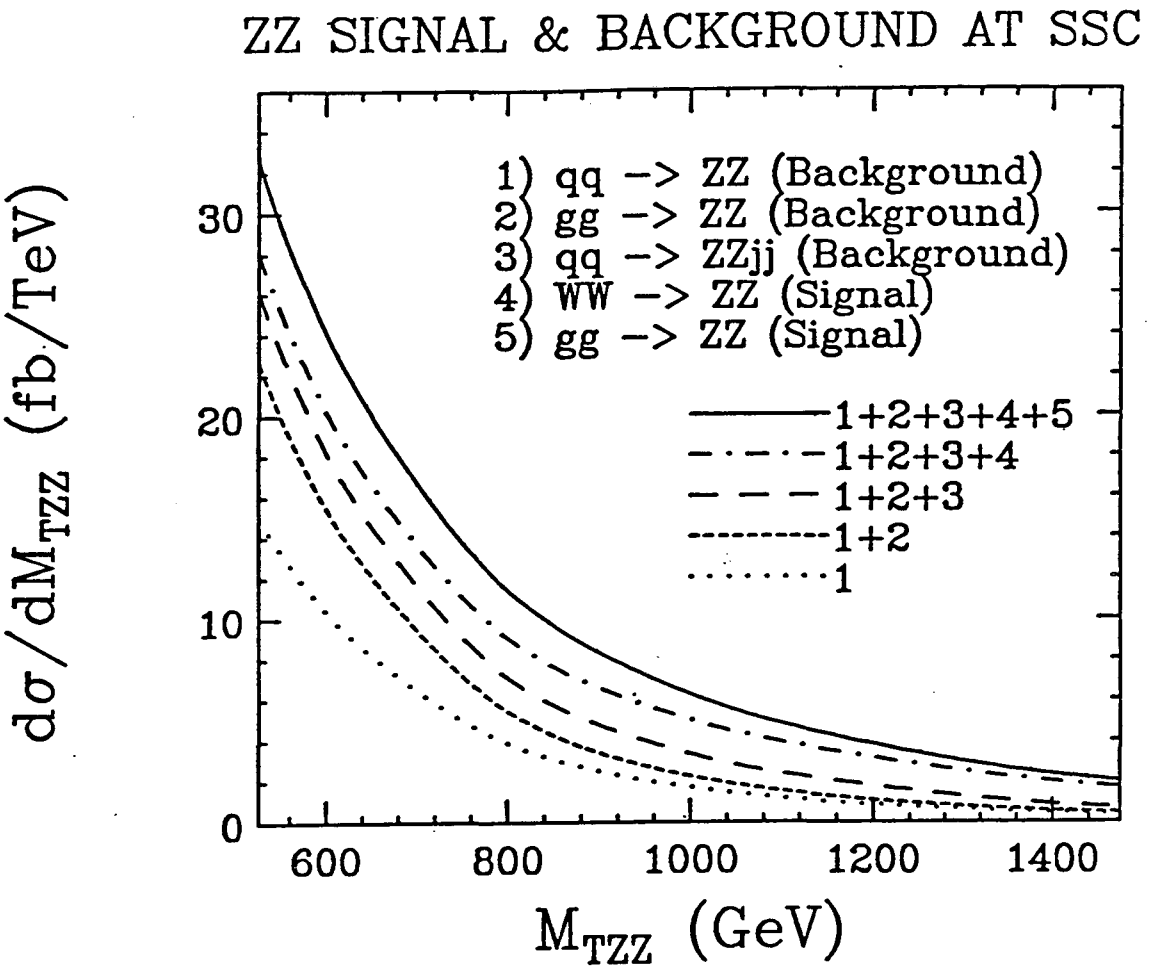

Figure 6.2 Signal and background components for ZZ final state at SSC with cuts and branching ratio as specified in the text.

were induced by condensates at different scales we would introduce correspondingly different cutoffs for WW and gg fusion.

6.2 Results for the "Linear Model"

We consider the decay channel[1,46,47] $ZZ \to e^+e^-/\mu^+\mu^- + \bar{\nu}\nu$, defined experimentally by an observed central Z with large transverse momentum recoiling against large missing transverse energy. The branching ratio is $BR = 0.025$, about 6 times larger than the four charged lepton decay mode to e's or μ's. (These results and those of the following section are from reference 7; they were computed with the EHLQ[34a] structure functions.)

We include three contributions to the background. The first is quark-antiquark

Table 6.1: Linear model signals and background in events per 10 fb^{-1} at SSC and LHC for various values of m_t. The statistical significance, $\sigma^{\uparrow,\downarrow}$, defined in Eqs. (3.19-3.20), is also shown. Cuts are $|y_\ell| < 2$ and $p_{T\ell} > 75$ GeV. For the SSC $M_{TZ} > 700$ GeV and for the LHC $M_{TZ} > 600$ GeV.

$\sqrt{s}$	m_t	Signal		Bkgd	$\sigma^\uparrow$	$\sigma^\downarrow$
TeV	GeV	gg	WW			
	100	4.1	17.3	29.4	4.0	3.0
40	150	10.1	17.3	30.3	5.0	3.6
	200	16.7	17.3	32.2	6.0	4.2
	100	0.75	1.83	8.98	0.9	0.8
16	150	1.72	1.83	9.11	1.2	1.0
	200	2.41	1.83	9.49	1.4	1.2

annihilation, $\bar{q}q \to ZZ$. The second[45] consists of the contributions to $gg \to ZZ$ that do not depend on the symmetry breaking sector, including production of $Z_T Z_T$ and $Z_T Z_L$ boson pairs as well as $Z_L Z_L$ pairs produced via the chirality-*nonflip* $\bar{t}t \to Z_L Z_L$ amplitude proportional to m_t^2. Third is the $O(\alpha_W^2)$ amplitude[48] for $qq \to qqZZ$. It and the $gg \to ZZ$ background are obtained from the standard model with a light Higgs boson, $m_H \leq 100$ GeV, just as we evaluated the α_W^2 amplitude background to the W^+W^+ signal in Section 5.1. The backgrounds were evaluated using the codes for the matrix elements of Glover and van der Bij[45] and of Baur and Glover.[48]

The signal and background for the SSC are plotted incrementally by component in figure 6.2 for $m_t = 150$ GeV. The differential cross section is shown with respect to the transverse ZZ mass, $M_{TZZ} = 2\sqrt{p_{TZ}^2 + M_Z^2}$, where p_{TZ} is the transverse momentum of the observed Z. The decay branching ratio $BR = 0.025$ is included. The lepton rapidity and transverse momentum cuts are $|y_l| < 2$ and $p_{Tl} > 75$ GeV. The gg fusion component of the signal is clearly substantial.

Table 6.1 exhibits event yields per 10 fb^{-1} at the SSC and LHC for $m_t = 100$, 150, and 200 GeV with cuts to optimize the statistical significance defined in Eqs. (3.19 - 3.20). Neither the Z detection efficiency,[35] $\simeq 95\%$, nor the additional $\simeq 15\%$ contribution of the four-charged lepton decay mode are included. The table is therefore a realistic representation of the acceptance corrected values when the four charge lepton mode is included, and we shall not modify our significance criterion Eqs. (3.18 - 3.22) as we did in Sections 4 and 5. At the SSC we find $\sigma^\uparrow \simeq 4$, 5, 6 for $m_t = 100$, 150, 200 GeV, which would be diminished by 1, 2, and 3 respectively

if the gg fusion component of the signal did not contribute. The signal:background ratio is approximately 1:1, so that our "systematic error" criterion Eq. (3.18) is just satisfied. Consequently a 30% systematic uncertainty in the background would not overwhelm the signal.

The LHC signals for 10 fb^{-1} are not statistically significant. For $m_t = 150$ GeV a luminosity increase by a factor $(5.0/1.2)^2 = 17$ would bring statistical parity with the SSC for $\sigma^\dagger$. But for the cuts in Table 1 the LHC signal:background is between 1:4 and 1:2, so that Eq. (3.18) is violated. Raising the lepton transverse momentum cut from 75 to 200 GeV increases the signal:background to nearly 1:1 but with a factor 4.5 loss in signal. The LHC would then achieve a value of $\sigma^\dagger$ equal to that of the SSC if the luminosity were increased by a factor 35: for 350 fb^{-1} the LHC has 27.7 signal and 30.8 background events, very similar to the SSC values in Table 1 for 10 fb^{-1}. The remaining question is whether the measurements are actually feasible with good efficiency at such high luminosity. In addition to instrumental issues the background from Z + *jets* requires attention (see Barnett et al.[47]).

6.3 A Two Condensate Model

Though it has not been considered in the context of dynamical symmetry breaking with $\mathcal{L}_5$ strong, it is possible that two different condensates generate the W and fermion masses. That is, one large condensate can contribute most of the W mass while making no contribution to the fermion masses. A second smaller condensate can generate all of the fermion masses while making only a small contribution to the W mass. By isolating the WW and gg fusion components of the ZZ signal we can separately probe the mass scales of the W boson and fermion mass generating condensates, i.e., the mass scales of the quanta that form the respective condensates. I will illustrate this possibility with a model in which the W mass is generated dynamically by a strong $\mathcal{L}_5$ while the fermion masses are due to the smaller condensate of a light Higgs boson. Unfortunately, since there are no really attractive models of fermion mass generation, this model is not much more peculiar than any other.

Suppose for instance that M_W arises from minimal $SU(2)$ technicolor with one techniquark weak doublet, and that there is no Extended Technicolor sector to link the technicolor condensate to the quark-lepton sector. Suppose also there is a light Higgs boson, H', with $m_{H'} \lesssim 100$ GeV and that the top quark mass is $m_t = 150$ GeV. Let us also suppose that the $H'\bar{t}t$ Yukawa coupling is as big as we can conscionably

make it, say

$$\frac{y_t^2}{4\pi^2} = 1. \tag{6.4}$$

(The original Yukawa coupling constant, for pion-nucleon interactions, is actually five times bigger.) The values of m_t and y_t then require the vacuum expectation value of H' to be

$$v' = 25 \text{ GeV} \tag{6.5}$$

from which we find the technicolor contribution

$$v_{TC} = \sqrt{246^2 - 25^2} = 245 \text{ GeV}. \tag{6.6}$$

The H' production cross section at LEP is then reduced by a factor

$$\left(\frac{v'}{246 \text{ GeV}}\right)^2 = \frac{1}{100}, \tag{6.7}$$

so that there are no effective limits from LEP on the existence of H'. The complex H' weak doublet must be coupled to the technicolor sector to give mass to what would otherwise be a pair of charged Goldstone bosons. The H' would not be an easy object to find. It is amusing to think about how to search for it.

Suppose the $WW \to ZZ$ strong scattering due to the technicolor dynamics is represented by the linear model. In this model there is no gg fusion contribution to the ZZ signal. Then from table 6.1 we see that the 10 fb^{-1} signal at the SSC is just 17.3 events over a background of 30.3. The total 47.6 events is then only as big as a 1.33σ downward fluctuation of the 57.7 event total predicted by the conventional one-condensate model, including the 10.1 gg fusion events. Furthermore, the two condensate model yield has $\sigma^{\uparrow} = 3.1$ and $\sigma^{\downarrow} = 2.5$, so none of the significance criteria Eqs. (3.18 - 3.22) are met.

However experiments at the SSC are also preparing for luminosity above the initial 10^{33} cm^{-2} sec^{-1} design value.[49] In addition to more robust discovery signals, higher luminosity would allow more detailed analysis of the signal, as in the present example. In order for the difference between the one and two condensate models to be separated by a 3σ fluctuation of the one condensate model prediction, the luminosity must be increased by $(3/1.33)^2 = 5.1$ to 50 fb^{-1} . At that luminosity the statistical significance of the two condensate model would be $\sigma^{\uparrow} = 7.1$ and $\sigma^{\downarrow} = 5.7$, well in excess of the minimal criterion Eqs. (3.21 -3.22), but with the specified cuts it would not meet the "systematic error" criterion Eq. (3.18). By the time of high luminosity running we will have a better understanding of the background so that it should be possible to relax Eq. (3.18). It may also be possible to use double[50] or single[51]

jet tagging to separate the gg and WW components, since there are no quark jets associated with gg fusion. The rapidity gaps associated with WW fusion but not with gg fusion could provide another means to separate the two mechanisms.[52]

It is unlikely that this measurement could be done at the LHC. A 3σ separation of the two-condensate model signal from the prediction of the one condensate model would require 390 fb^{-1} . Even with that luminosity the two condensate model signal — 71 signal events over a background of 350 implying $\sigma^{\uparrow} = 3.8$ and $\sigma^{\downarrow} = 3.4$ — would not meet the statistical criterion Eq. (3.21). To achieve $\sigma^{\uparrow} = 5$ for the two-condensate model at the LHC would in fact require 670 fb^{-1} . Furthermore, that signal is only 20% as big as the background. Raising the cuts to increase the signal:background ratio to resemble the SSC ratio would increase the required luminosity by about another factor of two.

7. Conclusion

The results presented suggest that the prospects are excellent at the SSC with its 10^{33} cm^{-2} sec^{-1} design luminosity to see the manifestations of electroweak symmetry breaking by a strong fifth force. In models with a prominent vector meson resonance analogous to the $\rho(770)$, the complementarity of resonant and nonresonant signals in the WZ and W^+W^+ channels implies that a signal will be seen in at least one channel if not both. More generally for any strong symmetry breaking dynamics the absence of visible resonances implies weaker exchange forces in all channels and in the W^+W^+ channel in particular. Then "gentle" unitarization models, that only gradually modify the threshold behavior dictated by the low energy theorems, will apply. These models provide big signals in the W^+W^+ channel which can be observed at the SSC with 10 fb^{-1} , far in excess of the minimum significance criterion, Eqs. (3.18 - 3.22).

After the initial observations of the manifestations of $\mathcal{L}_5$, the SSC will also have the capability with increased luminosity in the 10^{34} cm^{-2} sec^{-1} range to begin the program of detailed studies that will be needed regardless of what form the initial discovery may take. Even if $\mathcal{L}_5$ contains nothing but light Higgs bosons we will not be able to study it in sufficient detail with the 10 fb^{-1} data sample. Higher luminosity will be needed to study the production and decay properties in order to develop and confirm our understanding of the underlying theory. Likewise the first manifestations of a strong $\mathcal{L}_5$, e.g., in W^+W^+ scattering, will provide little more than the knowledge that we have discovered a new strong force. Experiments at 10^{34} cm^{-2} sec^{-1} at the SSC will then begin the study of the dynamics and associated spectrum.

At lower energy colliders both the signals and the signal:background ratios are smaller. In principle high luminosity can compensate to some extent though careful study is needed to determine what is actually possible in practice. The results presented here are idealized in that they do not consider at all the real world consequences of high luminosity such as the effect of event pile-up on the background estimates. Backgrounds that are under control at 10^{33} cm^{-2} sec^{-1} can be problematic at higher luminosity. Two examples are spurious missing energy backgrounds to $ZZ \to ll + \bar{\nu}\nu$ and the effect of particles arising from pile-up on the isolation of the leptons from W decay that is crucial to reject the top quark background in the W^+W^+ channel. There will be similar issues for second generation studies at the SSC with high luminosity.

At the idealized level of the calculations we saw in Section 6 that the LHC would require 350 fb^{-1} to obtain a minimally significant signal for the ZZ final state in the linear model, compared to 10 fb^{-1} at the SSC. It is unlikely that the LHC could distinguish the two condensate model ($\gtrsim$ 1000 fb^{-1} would be needed) that can be resolved at the SSC with 50 fb^{-1} . The least visible ρ_{TC} meson, at 2.52 TeV, required 160 fb^{-1} for a minimal signal at the LHC, which could be obtained at the SSC with 10 fb^{-1} . In the W^+W^+ channel the largest (no-CJV) signal, from the linear model, would meet the minimum criterion with $\sim$ 55 fb^{-1} , while 200 fb^{-1} are required for a signal equivalent to the 10 fb^{-1} SSC signal. The study of complementarity in the ρ chiral Lagrangian model provides one of the most encouraging results: with 100 fb^{-1} the LHC signals meet the minimum significance criterion in one of the two channels ($W^{\pm}Z$ or W^+W^+) for each of the three values of M_ρ considered.

Whether $\mathcal{L}_5$ describes a light Higgs boson or strong TeV-scale dynamics, the initial discovery will only be the first step on a long road. The first observations will not begin to provide the detailed information that will be required. A process lasting many decades at least will be needed. If the new physics involves a strong interaction, the enormous scale of the experimental facilities suggests the process will be far more lengthy and arduous than the road to QCD. The LHC will be a significant facility for the first step on that road. The SSC will enable the first step with a greater margin of confidence, and is in addition a long term investment in the future program that must follow. Unlike the classical physicists in the last years of the 19'th century who thought that physics had come to an end, in the last years of the 20'th century we can see that it is only just beginning.

Acknowledgements: I wish to thank Bill Kilgore for collaborating in the study of the rho chiral Lagrangian.

References

1. M.S. Chanowitz and M.K. Gaillard, *Nucl. Phys.* **B261** (1985) 379.

2. M. Soldate and R. Sundrum, *Nucl. Phys.* **B340** (1990) 1; R.S. Chivukula, M.J.Dugan, and M. Golden, BUHEP-92-18, 1992; R.S. Chivukula and M. Golden, *Phys. Lett.* **267B** (1991) 233; S.G. Naculich and C.P. Yuan, JHU-TUPAC-9200017,1992.

3. M.S. Chanowitz, M. Golden, and H.M. Georgi, *Phys. Rev.* **D36** (1987) 1490; *Phys. Rev. Lett.* **57** (1986) 2344.

4. V. Barger, K. Cheung, T. Han, and R. Phillips, *Phys. Rev.* **D42** (1990) 3052.

5. D. Dicus, J. Gunion, and R. Vega, *Phys. Lett.* **258B** (1991) 475; D. Dicus, J. Gunion, L. Orr, and R. Vega, UCD-91-10, 1991.

6. M. Berger and M.S. Chanowitz, *Phys. Lett.* **263B** (1991) 509.

7. M. Berger and M.S. Chanowitz, *Phys. Rev. Lett.* **68** (1992) 757.

8. M. Weinstein, *Phys. Rev.* **D8** (1973) 2511.

9. S. Weinberg, *Phys. Rev.* **D13** (1976) 974; **D19** (1979) 1277.

10. L. Susskind, *Phys. Rev.* **D20** (1979) 2619.

11. J.M. Cornwall, D.N. Levin, and G. Tiktopoulos, *Phys. Rev.* **D10** (1974) 1145.

12. C.E. Vayonakis, *Lett. Nuovo Cim.* **17** (1976) 383.

13. B.W. Lee, C. Quigg, and H. Thacker, *Phys. Rev.* **D16** (1977) 1519.

14. M.S. Chanowitz, M.A. Furman, and I. Hinchliffe, *Nucl. Phys.* **B153** (1979) 402.

15. G. Gounaris, R. Kögerler, and H. Neufeld, *Phys. Rev.* **D34** (1986) 3257; D. Soper and Z. Kunzst, *Nucl. Phys.* **D296** (1988) 253.

16. H. Veltman, *Phys. Rev.* **D41** (1990) 2294.

17. J. Bagger and C. Schmidt, *Phys. Rev.* **D41** (1990) 264.

18. W. Kilgore, LBL-32113, 1992.

19. H-J. He, Y-P. Kuang, and X-Y. Li, TUIMP-TH-92/47, 1992.

20. S. Weinberg, *Phys. Rev. Lett.* **17** (1966) 616.

21. T.D. Lee and C.N. Yang, *Phys. Rev. Lett.* **4** (1960) 307.

22. B.L. Ioffe, L.B. Okun, and A.P. Rudik, *Sov. Phys.* JETP *Lett.* **20** (1965) 128.

23. M.S. Chanowitz and M.K. Gaillard, *Phys. Lett.* **142B** (1984) 85; S. Dawson, *Nucl. Phys.* **B29** (1985) 42; G. Kane, W. Repko, and B. Rolnick, *Phys. Lett.* **148B** (1984) 367.

24. G. Altarelli, B. Mele, and F. Pitolli, *Nucl. Phys.* **B287** (1987) 205.

25. S. Weinberg, *Phys. Rev.* **166** (1968) 1568.

26. J. Gasser and H. Leutwyler, *Ann. Phys.* **158** (1984) 142.

27. K. Kawarabayashi and M. Suzuki, *Phys. Rev. Lett.* **16**(1960)255; Riazuddin and Fayyazuddin, *Phys. Rev.* **147**(1960)1071.

28. J. Donoghue, C. Ramirez, and G. Valencia, *Phys. Rev.* **D38** (1988) 2195.

29. M.S. Chanowitz and M. Golden, *Phys. Rev. Lett.* **61** (1985) 1053; E **63** (1989) 466.

30. K. Hikasa and K. Igi, *Phys. Rev.* **D261** (1991) 285.

30a O. Cheyette and M.K. Gaillard, *Phys. Lett.* **197B**(1987) 205.

30b M. Golden, *Beyond the Standard Model*, (Ames 1988) (QCD161:B47: 1988) p. 111.

31. J. F. Donoghue, C. Ramirez, and G. Valencia, *Phys. Rev.* **D39** (1989)1947; J. F. Donoghue and C. Ramirez, *Phys. Lett.* **234B** (1990)361.

32. A.Dobado, M.J.Herrero, and J.Terron, *Z. Phys.* **C50** (1991)205, 465; A.Dobado, M.J.Herrero, and T.N.Truong, *Phys. Lett.* **235B** (1990)102, 134.

33. S.Dawson and G.Valencia, *Nucl. Phys.* **B352** (1991)27; J.Bagger, S.Dawson, and G.Valencia, FERMILABPUB-92-75-T, 1992.

34. R.N. Cahn et al., *Experiments, Detectors, and Experimental Areas for the Supercollider*, eds. R. Donaldson and M. Gilchriese (World Scientific, Singapore, 1987) p.187.

34a E.Eichten et al., *Rev. Mod. Phys.* **56** (1984) 579.

35. Solenoidal Detector Collaboration, E.L. Berger et al., *Technical Design Report*, SDC-92-201, 1992.

36. D. Dicus and R. Vega, *Phys. Lett.* **217B** (1989) 194.

37. D. Dicus and R. Vega, *Nucl. Phys.* **B329** (1990) 533.

38. J. Thomas and E. Wang, in preparation.

39. M. Berger and M.S. Chanowitz, *Phys. Lett.* **267B** (1991) 416.

40. W.Hoogland et al., *Nucl. Phys.* **B69** (1974) 266; J.Baton et al., *Phys. Lett.* **33B** (1970) 525, 528; J.Prukop et al., *Phys. Rev.* **D10** (1974) 2055; D.Cohen et al., *Phys. Rev.* **D7** (1973) 662.

41. J. Bagger, S. Dawson, and G. Valencia, *Phys.Rev. Lett.* **67** (1991) 2256.

42. H.M. Georgi et al., *Phys. Rev. Lett.* **40** (1978) 62.

43. R.N. Cahn and S. Dawson, *Phys. Lett.* **136B** (1984) 196.

44. The unitarity constraint from Eq. (6.2) is correspondingly weaker. See T. Appelquist and M.S. Chanowitz, *Phys. Rev. Lett.* **59** (1987) 2405.

45. E.W.N. Glover and J.J. van der Bij, *Nucl. Phys.* **B321** (1989) 561.

46. R.N. Cahn and M.S. Chanowitz, *Phys. Rev. Lett.* **56** (1327) 1986.

47. R.M. Barnett, K. Einsweiler, and I. Hinchliffe, SSC-SDC Report 90-00099, 1990.

48. U. Baur and E.W.N. Glover, *Nucl. Phys.* **B347** (1991) 12; V. Barger et al., *Phys. Rev.* **D44** (1991) 1426.

49. *Site Specific Conceptual Design Report*, ed. J. Sanford, SSC-SR-1051, 1990.

50. R.N. Cahn et al., *Phys. Rev.* **D35** (1987) 1126; R. Kleiss and W.J. Stirling,*Phys. Lett.* **200B** (1988) 193.

51. V. Barger et al., ref. 48.

52. J. D. Bjorken, SLAC-PUB-5616, 1992.

LAWRENCE BERKELEY LABORATORY
UNIVERSITY OF CALIFORNIA
INFORMATION RESOURCES DEPARTMENT
BERKELEY, CALIFORNIA 94720